Role of the Ndc1 interaction network in yeast nuclear pore complex assembly and maintenance

Evgeny Onischenko,[1] Leslie H. Stanton,[1] Alexis S. Madrid,[1] Thomas Kieselbach,[2] and Karsten Weis[1]

[1]Department of Molecular and Cell Biology, Division of Cell and Developmental Biology, University of California, Berkeley, Berkeley, CA 94720
[2]Department of Chemistry, Umeå University, 90187 Umeå, Sweden

The nuclear pore complex (NPC) mediates all nucleo-cytoplasmic transport, yet its structure and biogenesis remain poorly understood. In this study, we have functionally characterized interaction partners of the yeast transmembrane nucleoporin Ndc1. Ndc1 forms a distinct complex with the transmembrane proteins Pom152 and Pom34 and two alternative complexes with the soluble nucleoporins Nup53 and Nup59, which in turn bind to Nup170 and Nup157. The transmembrane and soluble Ndc1-binding partners have redundant functions at the NPC, and disruption of both groups of interactions causes defects in Ndc1 targeting and in NPC structure accompanied by significant pore dilation. Using photoconvertible fluorescent protein fusions, we further show that the depletion of Pom34 in cells that lack *NUP53* and *NUP59* blocks new NPC assembly and leads to the reversible accumulation of newly made nucleoporins in cytoplasmic foci. Therefore, Ndc1 together with its interaction partners are collectively essential for the biosynthesis and structural integrity of yeast NPCs.

Introduction

Exchange of macromolecules between the cytoplasm and the nucleus is mediated by dedicated transport channels in the nuclear envelope (NE) called nuclear pore complexes (NPCs). NPCs are embedded within NE at fusion sites between the inner and outer nuclear membrane. They are among the largest macromolecular assemblies in eukaryotic cells with an estimated mass of >50 MD (Hetzer et al., 2005; Tran, and Wente, 2006). The structural organization of NPC appears to be conserved in evolution and has been delineated in various systems using EM (Unwin, and Milligan, 1982; Hinshaw et al., 1992; Yang et al., 1998; Beck et al., 2004; Beck et al., 2007). However, no detailed molecular structure of NPC is currently available. A recent study combined a comprehensive proteomic analysis with a diverse set of biophysical data and computational modeling to propose a three-dimensional map of all *Saccharomyces cerevisiae* nuclear pore proteins (nucleoporins or Nups; Alber et al., 2007a,b). In addition, the first nucleoporin crystal structures have now been solved (Hodel et al., 2002; Berke et al., 2004; Weirich et al., 2004; Hsia et al., 2007; Jeudy, and Schwartz, 2007; Melcak et al., 2007; Schrader et al., 2008), leading to new

insight into NPC structure and organization (Hsia et al., 2007; Brohawn et al., 2008). Together, these studies have demonstrated that NPCs are constructed from ∼500 polypeptides, but because of their highly symmetric organization, NPCs consist of only ∼30 distinct nucleoporins, all present in 8, 16, or 32 copies per NPC (Rout et al., 2000; Cronshaw et al., 2002; Alber et al., 2007a,b). Despite our detailed knowledge of the protein composition of NPCs, little is known about the pathways that lead to NPC assembly, and it remains poorly understood how NPC biosynthesis is spatially or temporally coordinated. In higher eukaryotes that undergo an open mitosis, two NPC assembly pathways can be distinguished. The first pathway occurs upon completion of mitosis, when nucleoporin subcomplexes and membrane vesicles are recruited to chromatin during NE reformation (Rabut et al., 2004; Antonin et al., 2008; Dultz et al., 2008). In vitro studies using an NE assembly assay in *Xenopus laevis* egg extracts revealed discrete NPC assembly steps that are initiated by an early recruitment of the Nup107-160 complex (Belgareh et al., 2001; Harel et al., 2003; Walther et al., 2003) to chromatin by the DNA-interacting nucleoporin ELYS (embryonic large molecule derived from yolk sac)/Mel28 (Rasala et al., 2006; Franz et al., 2007; Gillespie et al., 2007). This is followed

The Rockefeller University Press $30.00
J. Cell Biol. Vol. 185 No. 3   475–491
www.jcb.org/cgi/doi/10.1083/jcb.200810030

JCB   **475**

THE JOURNAL OF CELL BIOLOGY

by the recruitment of membrane vesicles containing the transmembrane nucleoporins POM121 and NDC1, which in turn leads to the incorporation of Nup155 (Nup157/Nup170 in yeast) and Nup53 (Nup53/Nup59 in yeast) and ultimately to the formation of complete and functional NPCs (Antonin et al., 2008).

The second pathway occurs during interphase when new NPCs are synthesized and inserted into intact NEs (Maul et al., 1972; Winey et al., 1997; D'Angelo, and Hetzer, 2006). Little is known about the mechanism of NPC biogenesis in interphase, and it is unclear how NPCs are inserted into the two lipid bilayers of an intact NE. De novo NPC synthesis during interphase occurs in all eukaryotes, but many unicellular eukaryotes such as the yeast *S. cerevisiae* must rely exclusively on NPC insertion into intact double membranes as they undergo a closed mitosis with no NE breakdown. Transmembrane nucleoporins are thought to be crucial for interphase NPC biogenesis by anchoring and recruiting soluble NPC components to the nuclear membrane (Suntharalingam, and Wente, 2003; Antonin et al., 2008). In both mammalian and yeast cells, only three transmembrane nucleoporins have been characterized: POM121, gp210, and NDC1 in mammals and Pom34, Pom152, and Ndc1 in yeast (Wozniak, and Blobel, 1992; Hallberg et al., 1993; Wozniak et al., 1994; Chial et al., 1998; Rout et al., 2000; Mansfeld et al., 2006; Stavru et al., 2006a). In mammalian cells, RNAi-mediated silencing of POM121 alone or in combination with gp210 had no effect on cell viability but caused somewhat variable phenotypes with respect to the distribution of other nucleoporins (Antonin et al., 2005; Stavru et al., 2006b). RNAi depletion of NDC1, the only evolutionarily conserved transmembrane nucleoporin, caused more severe phenotypes and affected NE localization of multiple nucleoporins (Mansfeld et al., 2006; Stavru et al., 2006a). Interestingly, the knockout of NDC1 in *C. elegans* also affected nucleoporin distribution, but NDC1 is not absolutely essential for the viability of the animals (Stavru et al., 2006a), suggesting that the role of the three transmembrane nucleoporins in NPC biogenesis and maintenance might be redundant. In agreement with this, neither *POM152* nor *POM34* is essential for cell viability or NPC function in budding yeast. However, additional depletion of Ndc1 caused severe structural abnormalities of NPC and led to the appearance of enlarged pore structures within the NE (Madrid et al., 2006).

To better understand the role of transmembrane nucleoporins in NPC biogenesis, we identified the direct interaction partners of Ndc1 in budding yeast. We show that Ndc1 can be isolated in a subcomplex with Pom152 and Pom34 and that Ndc1 alternatively interacts with either Nup53 or Nup59. In turn, Nup53 and Nup59 directly bind to the core nucleoporins Nup170 and Nup157, thus establishing a connection between the core of NPC and the pore membrane. The removal of Ndc1-interacting partners leads to severe ultrastructural NPC defects resembling the enlarged pore phenotype observed upon depletion of Ndc1 in *pom152* deletion mutants (Madrid et al., 2006). Using the photoconvertible fluorescent protein Dendra (Gurskaya et al., 2006), we found that depletion of Pom34 in the absence of Nup53 and Nup59 leads to the reversible mislocalization of newly synthesized Nup82, indicating a block in the assembly

of new NPCs. Our results demonstrate critical but redundant roles of the Ndc1-interacting nucleoporins in the assembly and structural integrity of yeast NPCs.
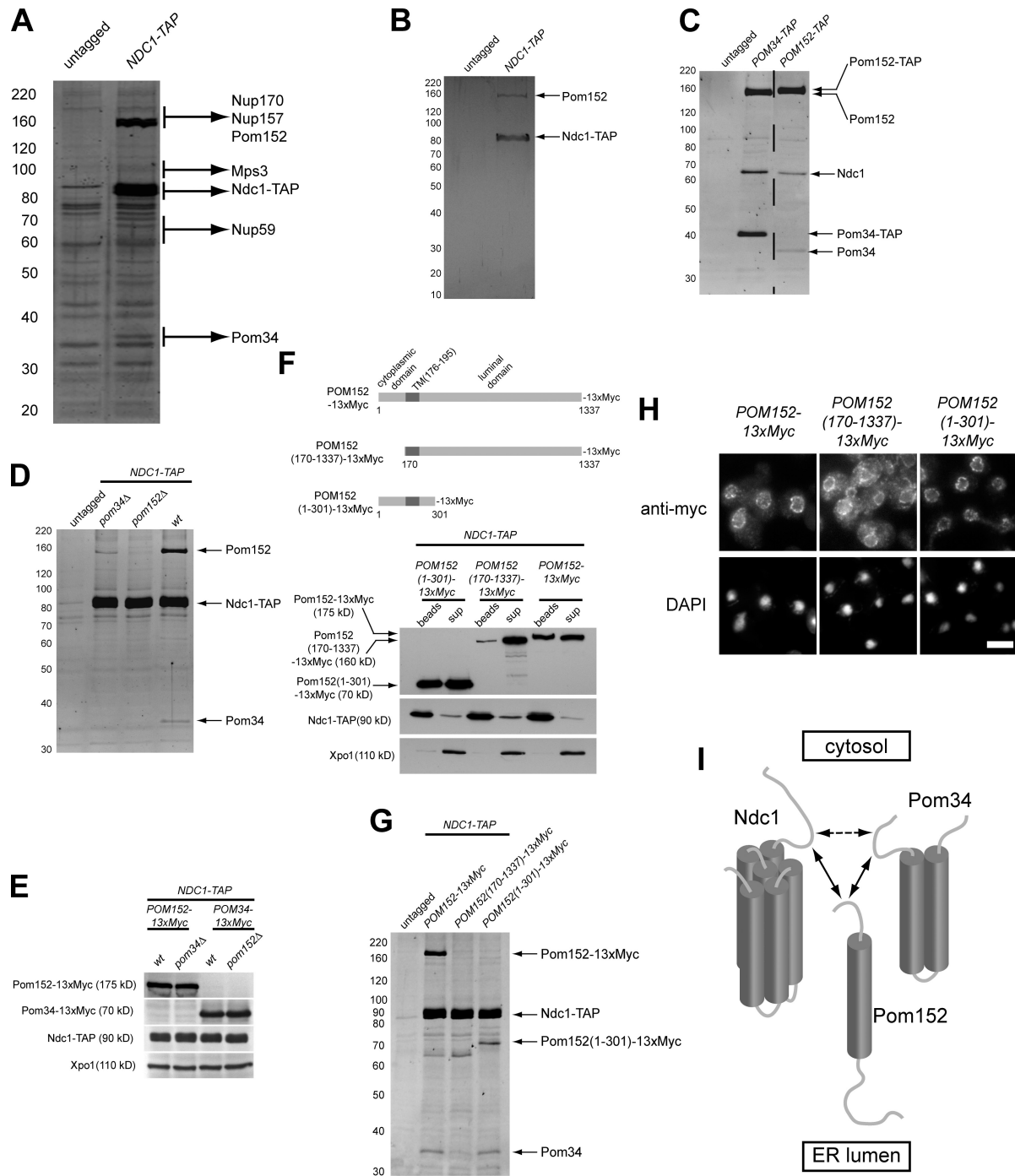
Results

### Identification of Ndc1-interacting proteins

To identify Ndc1-interacting proteins, we performed affinity purifications from yeast cells that express a tagged version of Ndc1. We prefractionated yeast extracts to obtain a membrane fraction from which Ndc1 was extracted with the detergent digitonin and then affinity purified. Liquid chromatography (LC)–mass spectrometry (MS)/MS and matrix-assisted laser desorption/ionization time of flight MS analysis of copurified proteins revealed that Ndc1 specifically interacts with five nucleoporins, Nup170, Nup157, Pom152, Nup59, and Pom34, as well as one transmembrane protein associated with the spindle pole body, Mps3 (Fig. 1 A; Wozniak et al., 1994; Aitchison et al., 1995; Marelli et al., 1998; Rout et al., 2000; Jaspersen et al., 2002). The presence of Mps3 in the pull-downs is consistent with Ndc1 being a shared component of the spindle pole body and NPC (Chial et al., 1998).

Ndc1, Pom34, and Pom152 form a novel NPC subcomplex

Recent studies provided a comprehensive overview of the interactions among all known yeast nucleoporins (Alber et al., 2007a,b). Our findings are consistent with these results, and all the nucleoporins that we found to copurify with Ndc1 were also identified as close neighbors in these studies (Alber et al., 2007a,b). However, whether the interactions between Ndc1 and these nucleoporins are direct or indirect had not been analyzed previously. We therefore decided to investigate the detailed interaction patterns of the identified proteins. Pom152 was the most abundant protein present in the Ndc1 purifications (Fig. 1 A), prompting us to test whether Ndc1 and Pom152 interact with each other directly. Interestingly, we found that in low ionic strength conditions, Ndc1 could be copurified together with Pom152 in the absence of any other detectable proteins (Fig. 1 B). We therefore conclude that Ndc1 and Pom152 are direct interaction partners. To further explore the nature of the interactions between the transmembrane nucleoporins, we generated yeast strains that endogenously expressed affinity-tagged versions of Pom152 and Pom34 and performed similar affinity purifications as described for Ndc1. We found that Pom152 coprecipitated Ndc1 and Pom34. Similarly, Pom34 pulled down Ndc1 and Pom152 in all cases in the absence of any major contaminating proteins (Fig. 1 C). Therefore, the three transmembrane nucleoporins form a complex with each other. Of note in Pom34 purifications, Pom152 was consistently more abundant than Ndc1. This is in agreement with the recent finding that Pom152 and Pom34 can be copurified in a complex (Alber et al., 2007a,b), suggesting a direct interaction between Pom152 and Pom34. To further examine the interaction relationships between Ndc1 and the other two transmembrane nucleoporins, we analyzed Ndc1 purifications in deletion mutants lacking either *POM34* or

Figure 1. **Identification of Ndc1-interacting proteins and characterization of the Ndc1 subcomplex.** (A) Affinity purification from yeast expressing TAP-tagged Ndc1 (*NDC1-TAP*) or untagged controls. Gel areas were excised and subjected to LC-MS/MS. Lines mark borders of areas subjected to MS analysis. (B) Profile of an Ndc1 affinity purification performed in low ionic strength conditions. (C) Comparison of purifications performed from cells expressing TAP-tagged versions of Pom34 (*POM34-TAP*), Pom152 (*POM152-TAP*), or untagged controls. (D) Comparison of Ndc1-TAP affinity purifications from wild-type (wt), *pom34Δ*, *pom152Δ*, or untagged control cells. For A–D, purified proteins were eluted, separated by SDS-PAGE, and visualized by SYPRO-Ruby. (E) Western blot analysis of the levels of myc-tagged Pom152 or myc-tagged Pom34 in wild-type, *pom34Δ*, or *pom152Δ* cells expressing Ndc1-TAP. Ndc1-TAP and Xpo1/Crm1 levels are used as loading controls. (F) Western blot analysis of Ndc1 purifications from cells expressing Ndc1-TAP together with either 13×myc-tagged Pom152$_{full-length}$, Pom152$_{170-1337}$, or Pom152$_{1-301}$. The scheme depicts the membrane topology of Pom152. Xpo1 was included as a control. sup, supernatant. (G) Comparison of Ndc1 purifications from cells expressing full-length Pom152-13×myc or its truncations. Proteins were visualized with SYPRO-Ruby. (H) Distribution of full-length Pom152 and its truncations tagged with 13×myc analyzed by immunofluorescence. Nuclei were stained with DAPI. (I) Model summarizing the interactions between Ndc1, Pom152, and Pom34. Solid arrows indicate direct protein interactions. The dashed arrow displays the functional requirement of Pom34 for the Ndc1 subcomplex integrity. Migration rate references for all gel image panels are shown in kilodaltons. Bar, 5 µm.
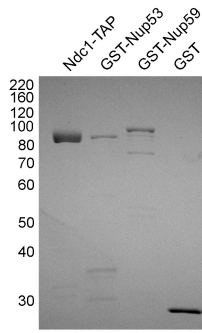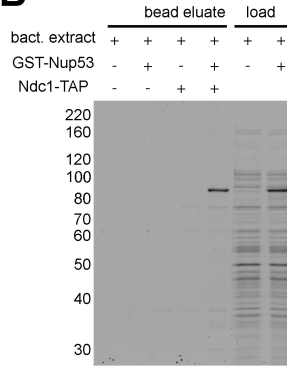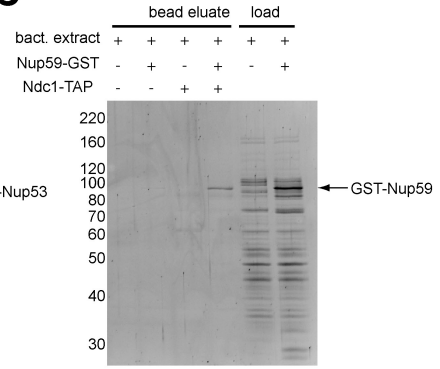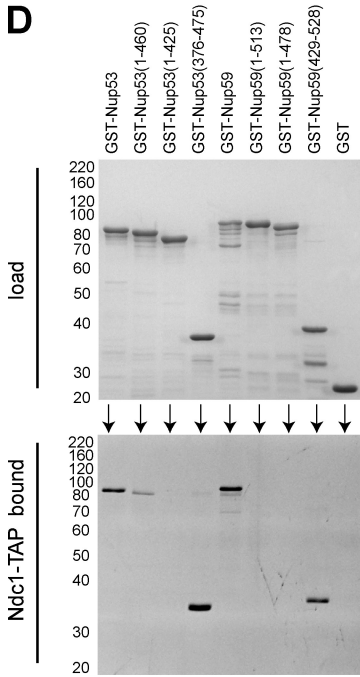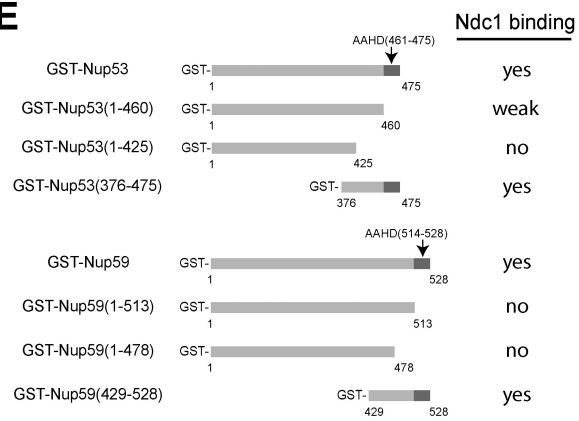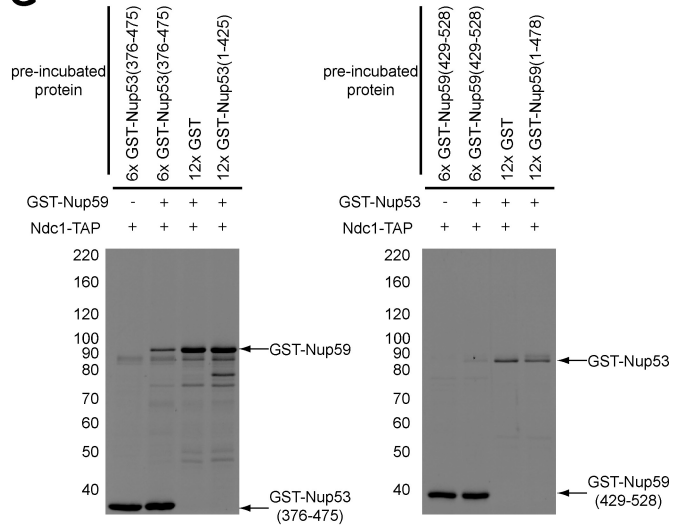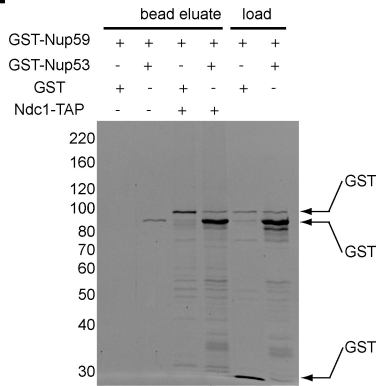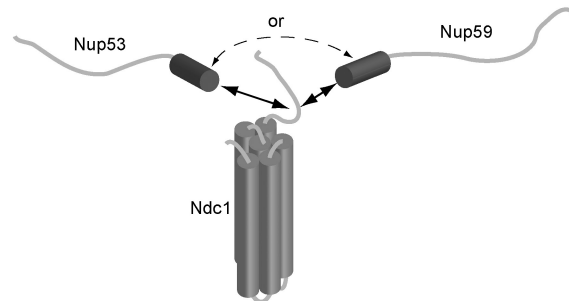
POM152. Interestingly, the deletion of *POM34* resulted in strongly reduced amounts of copurified Pom152, and similarly, the deletion of *POM152* severely diminished the amounts of Pom34 in Ndc1 purifications (Fig. 1 D). Because the deletion of one POM had no detectable effect on the expression of the other (Fig. 1 E), this indicates that the interactions between Ndc1, Pom152, and Pom34 are interdependent.

It was recently shown that Pom152 and Pom34 form a stable, ring-like structure, and it was proposed that this complex is stabilized by interactions involving the large luminal domain of Pom152 (Alber et al., 2007a,b). We therefore decided to test whether the interactions between Ndc1 and the two Poms are dependent on the luminal domain of Pom152. We performed Ndc1 purifications from yeast strains expressing truncated versions of myc-tagged Pom152. A C-terminal Pom152 truncation (Pom152$_{1-301}$), which lacks most of the luminal domain (Tcheperegine et al., 1999), was efficiently coprecipitated with Ndc1 and still supported the recruitment of Pom34. In contrast, an N-terminal truncation of Pom152 (Pom152$_{170-1,337}$), essentially lacking the entire cytosolic domain (Tcheperegine et al., 1999), did not copurify with Ndc1 and prevented efficient recruitment of Pom34 (Fig. 1, F and G). Consistent with this, Pom152$_{1-301}$ localized correctly to NE, whereas Pom152$_{170-1,337}$ did not (Fig. 1 H). This mislocalization of Pom152$_{170-1,337}$ was specific, and no effect on Ndc1 or Pom34 localization could be observed in these cells (Fig. S1 A). Of note, Pom152$_{170-1,337}$ was correctly inserted into the membrane as judged by its presence in the membrane fraction and by its detergent extractability (Tcheperegine et al., 1999; unpublished data).

Together, these findings indicate that all three yeast transmembrane nucleoporins form a distinct NPC subcomplex, which we refer to as the Ndc1 subcomplex. This complex is held together by at least two direct interactions: (1) between Ndc1 and Pom152 and (2) between Pom152 and Pom34. However, the overall integrity of the complex depends on the presence of both Poms and predominantly relies on interactions that occur on the cytosolic portions of these three transmembrane proteins (Fig. 1 I).

### Nup59 and Nup53 directly interact with Ndc1 and also bind directly to Nup157 and Nup170

To discriminate between direct and indirect interactions connecting Ndc1 to its other binding partners, we used in vitro binding approaches with purified proteins. First, we tested whether Ndc1 directly binds to Nup59. In this analysis, we also included the highly related Nup53, which was not detected in the original MS analysis (Fig. 1 A). Tandem affinity purification (TAP)–tagged Ndc1 was purified from yeast cells using S protein–conjugated agarose beads (S beads), whereas recombinant GST fusions of Nup53 and Nup59 were obtained from *Escherichia coli* (Fig. 2 A). To probe for direct binding, we incubated GST-Nup53 or GST-Nup59 fusion proteins premixed with *E. coli* extract (1:4 in total protein concentration) with Ndc1–S beads or with S beads alone and eluted bound proteins with high salt. Addition of *E. coli* extract was used to internally control for nonspecific binding interactions with Ndc1. We found that both GST-Nup53 and GST-Nup59 were specifically purified from the protein mixtures by Ndc1-coated beads (Fig. 2, B and C). These interactions did not depend on the presence of *E. coli* proteins and were not detected with GST alone (Fig. S1 B), demonstrating that both Nup59 and Nup53 directly and specifically bind to Ndc1.

Both Nup53 and Nup59 contain 15–amino acid-long amphipathic α-helical domains (AAHDs) at their C termini (Patel and Rexach, 2007), prompting us to test whether the AAHDs are important for Ndc1 binding. We created truncations of both Nup53 and Nup59 and tested them for binding to Ndc1. The removal of the last 15 amino acids completely abolished Nup59 binding to Ndc1 and severely impaired the binding of Nup53. Further deletion of the terminal 50 amino acids completely prevented the interactions of both proteins with Ndc1, demonstrating that the very C termini of Nup53 and Nup59 are necessary for the direct interaction with Ndc1 (Fig. 2, D and E). To examine whether these C-terminal domains are also sufficient for Ndc1 binding, we expressed GST fusion proteins containing the C-terminal 100 amino acids of Nup53 and Nup59. As shown in Fig. 2 (D and E), the short C-terminal fragments of both Nup53 and Nup59 efficiently interacted with Ndc1, which is comparable with full-length proteins.

Because Nup53 and Nup59 are homologous proteins that use similar C-terminal domains for Ndc1 binding, it was important to determine whether these two proteins use overlapping or distinct binding sites on Ndc1. To differentiate between these possibilities, Ndc1 beads were premixed either with a 10-fold molar excess of GST or with a 10-fold molar excess of GST-Nup53 and then incubated with GST-Nup59. As shown in Fig. 2 F, preincubation with an excess of GST-Nup53 caused a significant reduction in GST-Nup59 binding when compared with the GST control. Furthermore, the C terminus of Nup53 (Nup53$_{376-475}$) was sufficient to inhibit the interaction between Nup59 and Ndc1, whereas an N-terminal fragment of Nup53 lacking the AAHD (Nup53$_{1-425}$) had no effect (Fig. 2 G). Conversely, the interaction between Nup53 and Ndc1 was blocked when Ndc1-TAP beads were preincubated with an excess of the C-terminal 100 amino acids of Nup59 (GST-Nup59$_{429-528}$), but no inhibition was seen in the presence of a Nup59 variant that

---

Figure 2. **The interactions of Ndc1 with Nup53 and Nup59.** (A) Purified proteins separated by SDS-PAGE and stained with Coomassie brilliant blue. (B and C) SYPRO-Ruby–stained gels showing input (load) or eluates from S beads with immobilized Ndc1-TAP or S beads alone incubated with *E. coli* extract (bact. extract) or *E. coli* extract premixed with either GST-Nup53 or GST-Nup59. (D, top) Purified proteins stained with Coomassie brilliant blue. (bottom) SYPRO-Ruby–stained gel showing eluates from Ndc1-TAP beads after incubation with variants of Nup53 and Nup59. (E) Summary of interactions between truncations of Nup53 or Nup59 and Ndc1. (F) Binding of GST-Nup59 to Ndc1-TAP beads after preincubation with 10-fold excess of GST or 10-fold access of GST-Nup53. (G) Comparison of GST-Nup59 binding with Ndc1-TAP beads after preincubation with an excess of GST-Nup53 truncations or GST alone (left), or the reciprocal experiment with GST-Nup53 and an excess of GST-Nup59 truncations or GST alone (right). (H) Model summarizing the interactions between Ndc1 and Nup53 or Nup59. Solid arrows indicate direct protein interactions. Dashed arrow reflects the competition observed between Nup53 and Nup59 for Ndc1 binding. Migration rate references for all gel image panels are shown in kilodaltons.
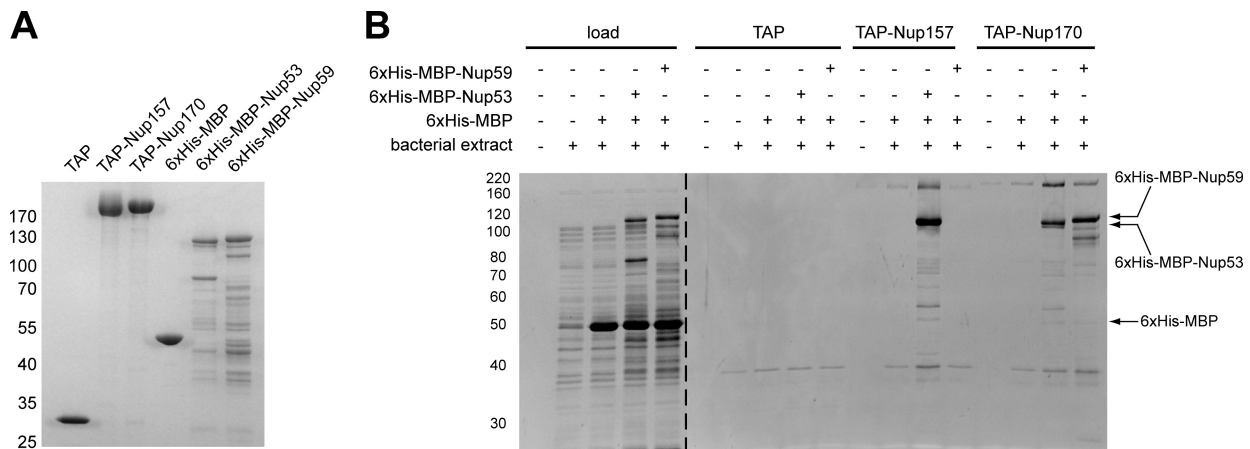
Figure 3. **The interactions between Nup53, Nup59, Nup157, and Nup170.** (A) Coomassie brilliant blue–stained gel showing samples of purified proteins. (B) SYPRO-Ruby–stained gel showing samples of the load (left) or eluates from TAP-Nup170, TAP-Nup157, or TAP beads after incubation with different mixtures of *E. coli* extract, 6×His-MBP-Nup53, 6×His-MBP-Nup59, or 6×His-MBP. Migration rate references for all gel image panels are shown in kilodaltons.

lacks the extreme C terminus (GST-Nup59$_{1–478}$; Fig. 2 G). These competition experiments show that Nup53 and Nup59 cannot bind to Ndc1 at the same time, suggesting that they use similar or overlapping binding sites. Furthermore, they support a model wherein Ndc1 forms two alternative complexes at the NPC, one with Nup53 and one with Nup59 (Fig. 2 H).

We next tested whether Ndc1 could also directly bind to Nup157 or Nup170, but our attempts to detect specific direct interactions between these proteins were not successful (unpublished data). This suggested that the interactions between Ndc1, Nup157, and Nup170 that we observed in Fig. 1 A might be indirect and mediated by bridging factors. Because Nup53 and Nup59 were previously shown to copurify with Nup170 (Marelli et al., 1998) and Nup170 shares high similarity with Nup157, we explored the pairwise binding interactions of Nup53 and Nup59 with Nup170 and Nup157. TAP-tagged fusions of full-length Nup157 and Nup170 or TAP-tagged alone were purified from yeast (Fig. 3 A) and tested for their ability to bind to maltose-binding protein (MBP) fusions of Nup53 or Nup59. We again included a mixture of *E. coli* proteins to internally control for binding specificity. Although Nup170 specifically purified both MPB-Nup53 and MBP-Nup59 from the protein mixtures, Nup157 only bound to MBP-Nup53 (Fig. 3 B and Fig. S1 C), suggesting that the interactions between these two pairs of proteins are not identical.

Collectively, our biochemical findings can be summarized in a model wherein Ndc1 displays a network of interactions at the most inner layer of NPC (see Fig. 9). First, Ndc1 is part of a complex that is formed by the three NPC transmembrane proteins, including Pom152 and Pom34. Second, Ndc1 forms complexes with either Nup53 or Nup59, which in turn recruit Nup157 or Nup170 to Ndc1 (see Fig. 9).

Nucleoporins interacting with Ndc1 are redundantly required for cell viability

Our biochemical analyses demonstrated that the interaction neighborhood of Ndc1 consists of four nucleoporins, Nup53, Nup59, Pom152, and Pom34. As a first step toward understand-

ing the functional significance of these interactions, we investigated the requirement of these proteins for cell viability. Previous work had shown that single deletions of *POM152*, *POM34*, *NUP53*, or *NUP59* and *pom152Δ pom34Δ* or *nup53Δ nup59Δ* double deletions are viable (Marelli et al., 1998; Madrid et al., 2006; Miao et al., 2006). Similarly, combined deletions of *NUP53* with either *POM34* or with *POM152* do not affect viability (Marelli et al., 1998; Miao et al., 2006; Table I). In contrast, cells containing deletions of *NUP59* together with either *POM152* or *POM34* are not viable (Table I; Marelli et al., 1998; Miao et al., 2006). We extended this analysis to all combinations of the four Ndc1-interacting nucleoporins using complete gene knockouts and conditional depletions using repressible *GAL* or *MET* promoters (Table I). This analysis confirmed that *NUP59* is essential for cell viability in the absence of either *POM152* or *POM34* independently of whether *NUP53* is present or not (Table I and Fig. S2 A). Similarly, using conditional alleles of *POM34* or *POM152* expressed under control of the *GAL* promotor, we observed that each of these nucleoporins is essential when both *NUP53* and *NUP59* are deleted (Table I and Fig. S2 B). These results indicate that two redundant functional elements exist among Ndc1-interacting proteins, Nup59 alone, and Pom152 together with Pom34. In addition, this analysis demonstrates that the essential role of these proteins is independent of Nup53 and that Nup53 is therefore functionally distinct from Nup59.

Targeting of Ndc1 to NE requires its interaction partners

The removal of the interaction partners of Ndc1 should affect the ability of Ndc1 to connect to the NPC. We therefore used the aforementioned conditional mutants to analyze whether the observed defects in cell viability are associated with an altered localization of Ndc1. We first tagged Ndc1 with a functional GFP tag in *pom152Δ pom34Δ nup53Δ* cells that conditionally express *NUP59* (Fig. S3). In the presence of Nup59, Ndc1 correctly localized to NE, but upon Nup59 depletion, it gradually mislocalized into the peripheral ER (Fig. 4 A, i; and Fig. S4 A). Importantly, this effect preceded any significant changes in cell

Table I. **Cell viability phenotypes in *POM152*, *POM34*, *NUP53*, and *NUP59* deletion and/or conditional expression mutants**

Genotype	Conditions	Viability	Reference
nup53Δ	NA	+	Marelli et al., 1998
nup59Δ	NA	+	Marelli et al., 1998
pom152Δ	NA	+	Marelli et al., 1998
pom34Δ	NA	+	Miao et al., 2006
nup53Δ nup59Δ	NA	+	Marelli et al., 1998
nup53Δ pom152Δ	NA	+	Marelli et al., 1998
nup53Δ pom34Δ	NA	+	Miao et al., 2006
nup59Δ pom152Δ	NA	−	Marelli et al., 1998
nup59Δ pom34Δ	NA	−	Miao et al., 2006
pom152Δ pom34Δ	NA	+	Miao et al., 2006
nup53Δ pom152Δ pom34Δ	NA	+	This study[a]
pom152Δ pom34Δ GAL-3×HA-NUP59	Galactose	+	This study[b]
pom152Δ pom34Δ GAL-3×HA-NUP59	Dextrose	−	This study[b]
nup53Δ pom152Δ pom34Δ MET3-3×HA-NUP59	No methionine	+	This study[b]
nup53Δ pom152Δ pom34Δ MET3-3×HA-NUP59	With methionine	−	This study[b]
nup53Δ nup59Δ GAL-3×HA-POM34	Galactose	+	This study[b]
nup53Δ nup59Δ GAL-3×HA-POM34	Dextrose	−	This study[b]
nup53Δ nup59Δ GAL-3×HA-POM152	Galactose	+	This study[b]
nup53Δ nup59Δ GAL-3×HA-POM152	Dextrose	−	This study[b]

NA, not applicable.

[a]Unpublished data.

[b]Characterization of the conditional mutants can be found in Fig. S2.

growth, indicating that the mislocalization of Ndc1 is not a secondary consequence of general cell malfunction (compare Fig. 4 A [i] with Fig. S2 C). Similarly, in *pom152Δ pom34Δ* cells, the depletion of Nup59 also resulted in partial mislocalization of Ndc1 (Fig. 3 A, c; and Fig. S2 C). However, in cells in which *POM152* and *POM34* were not deleted, the depletion of Nup59 did not cause mislocalization of Ndc1 either in the presence or absence of Nup53 (Fig. 4 A, ii and iv), demonstrating that the two Poms can compensate for the loss of Nup59.

To directly test whether the Poms function in Ndc1 targeting, we used *nup53Δ nup59Δ* cells, which express either of the POM genes in a conditional manner and examined the distribution of Ndc1 via GFP. In both cases, Ndc1 predominantly localized to NE in permissive conditions, although some faint peripheral ER localization was already apparent. However, upon shift to nonpermissive conditions, Ndc1 became gradually dispersed from NE (Fig. 4 B, i and iii). This redistribution coincided with the depletion of the respective Poms and started before pronounced defects in cell growth became apparent (compare Fig. 4 B [i and iii] with Fig. S2 D). No mislocalization of Ndc1 was observed in strains in which *NUP53* and *NUP59* were present (Fig. 4 B, ii and iv). Together, these results present evidence that the essential functions of Nup59 and the Poms tightly correlate with their role in targeting of Ndc1 to the NPC. Consistent with our biochemical findings, this also suggests that Nup59 and an intact Ndc1 subcomplex play a critical but redundant role in establishing the connections between Ndc1 and other core elements of NPC.

Ndc1-interacting nucleoporins play a key role in NPC structure and function

We have previously demonstrated that depletion of Ndc1 in yeast has severe consequences on NPC structure and function

(Madrid et al., 2006). To investigate the functional consequences accompanying the mislocalization of Ndc1 that we observed after the removal of its interaction partners, we modified the aforementioned strains to express GFP-tagged versions of various nucleoporins, including the cytoplasmic Nup82, the central Nup188 and Nup133, and the nuclear Nup2. To examine functional defects of NPC, we also monitored the localization of GFP fusions of the nuclear protein Npl3 or its variant Npl3(S411A), which has a weakened nuclear import activity (Siebel and Guthrie, 1996; Gilbert et al., 2001).

We first analyzed the effect of Nup59 depletion in *pom152Δ pom34Δ* strains either in the presence or absence of Nup53. As expected, in *pom152Δ pom34Δ* cells expressing Nup59, all four nucleoporins were properly localized (Fig. 5 A, left). However, upon Nup59 depletion, cells displayed a partial mislocalization of Nup82, Nup133, and Nup2 in foci that appeared to be associated with NE (Fig. 5 A, right). This localization defect correlated with a defect in NPC function because the sensitive nuclear import reporter Npl3(S411A)-GFP partially mislocalized to the cytoplasm (Fig. 5 A).

Interestingly, in *pom34Δ pom152Δ nup53Δ* cells conditionally expressing Nup59, defects in nucleoporin distribution were already evident even in permissive conditions (Fig. 5 B, left). Furthermore, these cells partially mislocalized the strongly imported Npl3 protein (compare Fig. 5 B [left] with Fig. S4 B), indicating that they have both structural and functional NPC defects. Upon depletion of Nup59, these defects were further exacerbated, as indicated by mislocalization of all four nucleoporins and the strong cytoplasmic mislocalization of Npl3-GFP (Fig. 5 B, right). Therefore, in the absence Pom152 and Pom34, both Nup53 and Nup59 become critical for the proper structural organization and function of NPC. However, their roles
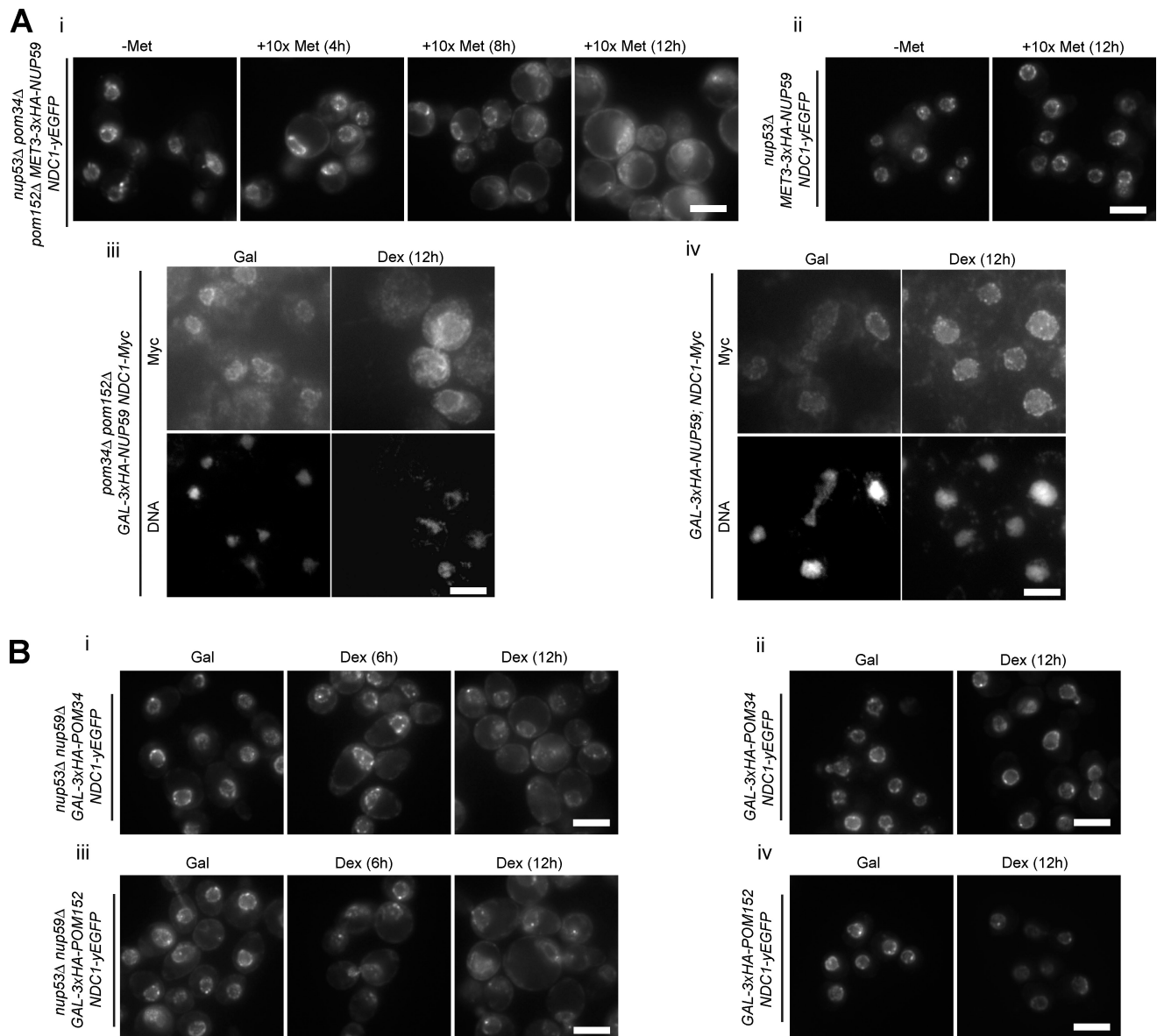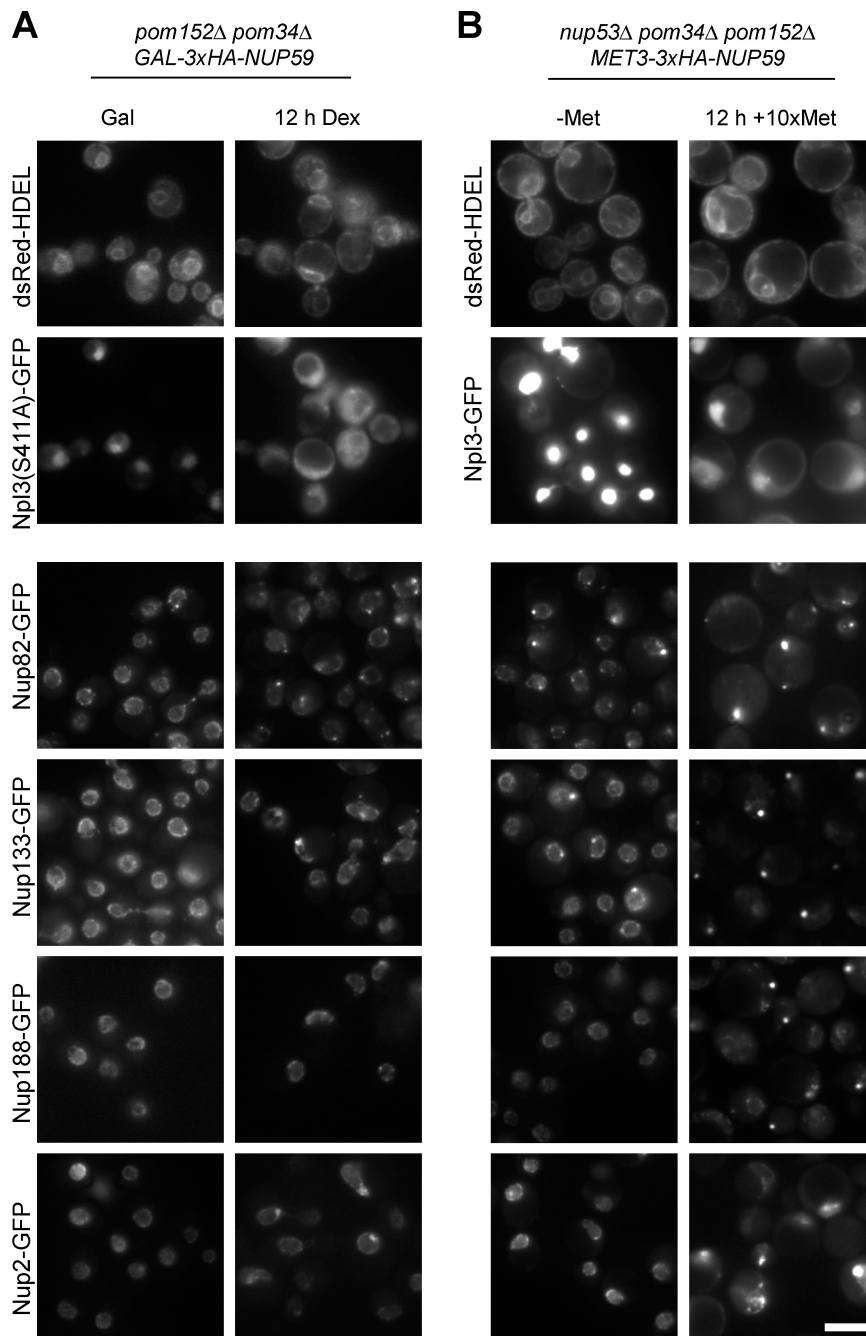
Figure 4. **The role of Pom152, Pom34, Nup53, and Nup59 in targeting of Ndc1 to NE.** (A) Localization of Ndc1 was compared in *nup53Δ pom34Δ pom152Δ MET3-3×HA-NUP59* (i), *nup53Δ MET3-3×HA-NUP59* (ii), *pom34Δ pom152Δ GAL-3×HA-NUP59* (iii), and *GAL-3×HA-NUP59* (iv) cells by fluorescence microscopy (via the yeast EGFP tag in i and ii) or by indirect immunofluorescence (via 13×myc tag in iii and iv) in permissive (galactose medium [gal] or medium lacking methionine [−met]) and nonpermissive conditions (dextrose-containing medium [dex] or medium containing 10× methionine [+10× met]). For immunofluorescence, cells were also stained with DAPI to label DNA. (B) Similar analysis of Ndc1–yeast EGFP localization in *nup53Δ nup59Δ GAL-3×HA-POM34* (i), *GAL-3×HA-POM34* (ii), *nup53Δ nup59Δ GAL-3×HA-POM152* (iii), and *GAL-3×HA-POM152* (iv). Bars, 5 μm.

are not entirely equivalent because only *NUP59* is synthetically lethal with *POM152* and *POM34*. In addition, Nup53 and Nup59 have partially redundant roles because we observed exacerbated functional and structural defects in the absence of both these nucleoporins as compared with the conditions when only one of them was absent. We next investigated the effects on nuclear pore organization in *nup53Δ nup59Δ* cells that conditionally express either *POM34* or *POM152* (Fig. 6). In permissive conditions, we did not observe major localization defects of the reporter nucleoporins in either of these strains (Fig. 6, A and B, left). The only exception was Nup82, which we found to mislocalize in the *GAL-3×HA-POM152* cells.

Because we did not observe this in the *GAL-3×HA-POM34* cells, this phenotype is likely a consequence of the high level of Pom152 that is expressed in the presence of galactose. This had no detectable consequence on NPC function, as the Npl3-GFP reporter efficiently accumulated within the nuclei of these cells (Fig. 6, A and B, left). However, upon depletion of either Pom34 or Pom152, *nup53Δ nup59Δ* cells displayed almost complete mislocalization of Nup82 and a partial mislocalization of the central nucleoporins Nup133 and Nup188 into cytoplasmic foci. At the same time, Nup2 appeared to localize normally. This redistribution of nucleoporins also coincided with a strong mislocalization of Npl3-GFP to the cytoplasm,

A

pom152Δ pom34Δ
GAL-3xHA-NUP59

Gal | 12 h Dex

dsRed-HDEL

Npl3(S411A)-GFP

Nup82-GFP

Nup133-GFP

Nup188-GFP

Nup2-GFP

B

nup53Δ pom34Δ pom152Δ
MET3-3xHA-NUP59

-Met | 12 h +10xMet

dsRed-HDEL

Npl3-GFP

Figure 5. **Roles of Nup53 and Nup59 in NPC organization and function.** (A and B) *pom152Δ pom34Δ GAL-3×HA-NUP59* (A) or *pom152Δ pom34Δ nup53Δ MET3-3×HA-NUP59* (B) cells expressing GFP-tagged Nup82, Nup133, Nup188, or Nup2 or nuclear import reporters Npl3-GFP (B) or Npl3(S411A)-GFP (A) together with the ER reporter dsRed-HDEL were analyzed by fluorescence microscopy in both permissive and nonpermissive conditions. Gal, galactose medium; dex, dextrose-containing medium; −met, medium lacking methionine; +10× met, medium containing 10× methionine. Bar, 5 μm.
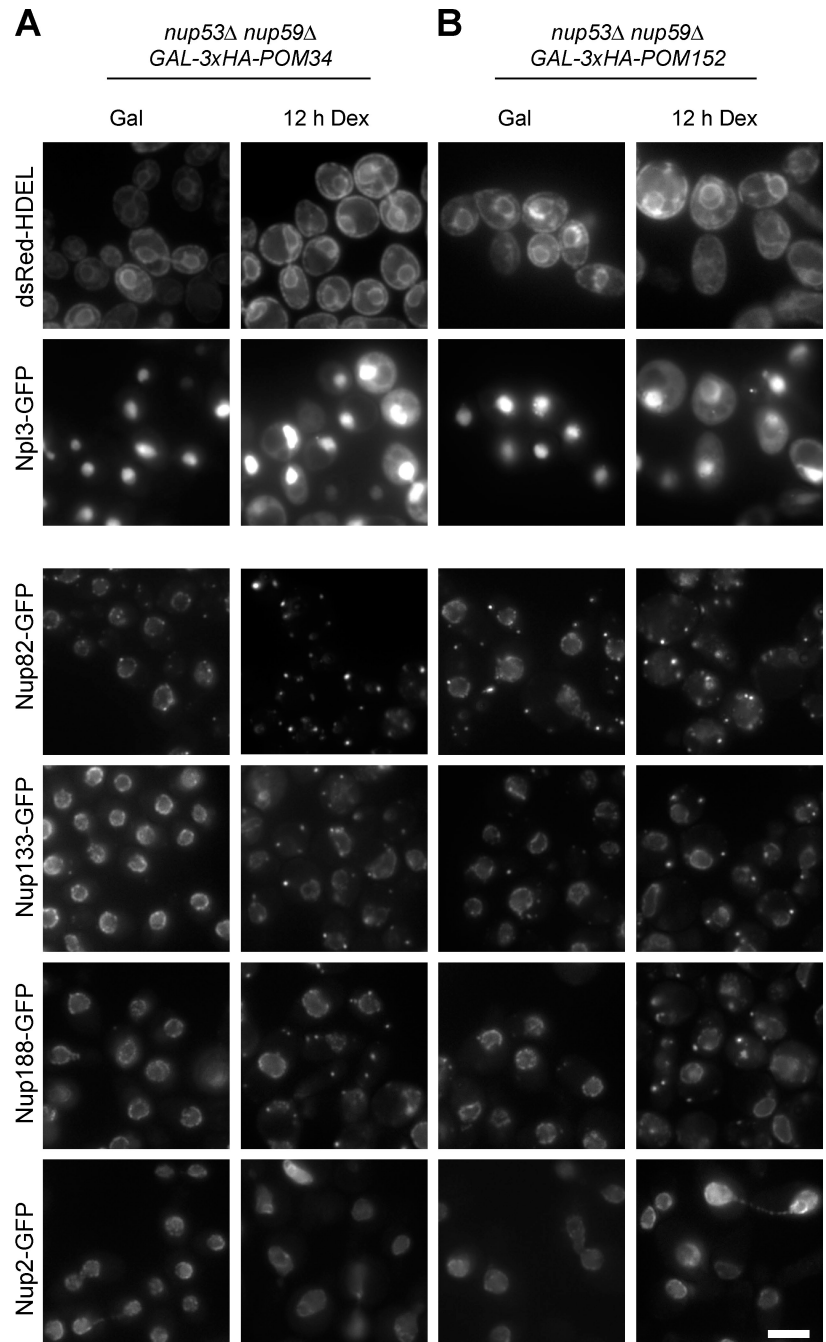
indicating impaired NPC function (Fig. 6, A and B, right). The similarity in the NPC phenotypes that we observed upon depletion of Pom152 or Pom34 indicates that these proteins cooperate to perform a similar function in the structural organization of NPC. Such cooperativity is consistent with our observations that the integrity of the Ndc1 subcomplex depends on both Pom152 and Pom34.

Ndc1-interacting proteins are important for the correct ultrastructural morphology of NPC

To examine the role of the Ndc1-interacting nucleoporins in the ultrastructural organization of NPCs, we analyzed the aforementioned mutant strains by transmission EM (McDonald and

Muller-Reichert, 2002). As expected, *pom152Δ pom34Δ GAL-NUP59* cells grown in permissive conditions displayed no obvious NPC defects (Fig. 7 A, i). However, upon Nup59 depletion, *pom152Δ pom34Δ* cells contained a large fraction of NPCs that had an increase in pore size (Fig. 7, A [ii] and B [i]). A similar pore dilation phenotype could be also observed in *pom152Δ pom34Δ nup53Δ MET3-3×HA-NUP59* cells even in the presence of Nup59, which is consistent with our fluorescence microscopy analysis (Fig. 5 B, left). Interestingly, upon depletion of Nup59, the NPC defects became significantly enhanced, and in addition to enlarged pores, we also observed large openings in NE that apparently lack electron-dense material (Fig. 7, A [iv and v] and B [ii]) reminiscent to the phenotype we had previously observed in *pom152Δ* cells after the depletion of Ndc1

Figure 6. **Roles of Pom152 and Pom34 in NPC organization and function.** (A and B) Fluorescence analysis as described in Fig. 5 in *nup53Δ nup59Δ* cells conditionally expressing Pom34 (A) or Pom152 (B). Gal, galactose medium; dex, dextrose-containing medium. Bar, 5 µm.

A *nup53Δ nup59Δ* GAL-3xHA-POM34

B *nup53Δ nup59Δ* GAL-3xHA-POM152

Gal | 12 h Dex | Gal | 12 h Dex

dsRed-HDEL

Npl3-GFP

Nup82-GFP

Nup133-GFP

Nup188-GFP

Nup2-GFP

(Madrid et al., 2006). A similar EM analysis in *nup53Δ nup59Δ* cells that conditionally expressed *POM34* did not reveal obvious NPC defects in either permissive or nonpermissive conditions (Fig. 7, A [vi and vii] and B [iii]). However, quantitative comparison of the mean number of pore structures at NE showed that these cells had a significant reduction in pore number and contained only approximately half the number of NPCs per nuclear section (Fig. 7 B, vi).

These observations show that the structural and functional NPC defects, which we have observed upon removal of various Ndc1-interacting proteins by fluorescence microscopy (Figs. 5 and 6), are accompanied by distinct changes in the ultrastructural morphology of NPCs or by a reduction in pore number.

Depletion of Pom34 results in a reversible mislocalization of newly synthesized Nup82 in *nup53Δ nup59Δ* cells

The depletion of Pom34 in *nup53Δ nup59Δ* cells resulted in nucleoporin mislocalization (Fig. 6 A), yet our EM analysis did not reveal obvious NPC defects. However, these cells displayed a significant reduction in pore number (Fig. 7). We were therefore interested to investigate whether the mislocalized nucleoporins represent newly synthesized proteins that fail to be incorporated into NPCs or whether they are derived from previously existing NPCs that have disintegrated. To address this question, we developed an assay to monitor the fate of old, already assembled NPCs as well as the assembly of new NPCs.
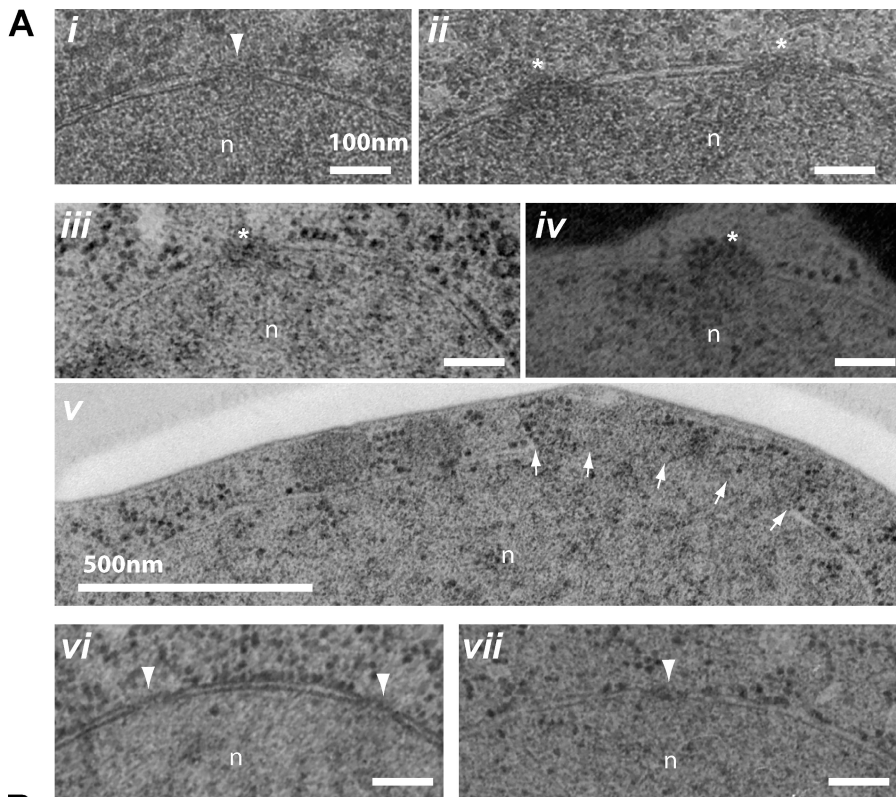
Figure 7. **Transmission EM analysis of NPC morphology in conditional mutants affecting Ndc1-interacting nucleoporins.** (A) NPCs (arrowheads) in *pom152Δ pom34Δ GAL-3×HA-NUP59* cells in permissive conditions (i) did not display morphological abnormalities. (ii) After incubation in nonpermissive conditions, a large fraction of dilated pores often displaying fuzzy electron-dense material could be detected (asterisks). (iii) A similar phenotype was observed in *pom152Δ pom34Δ nup53Δ MET3-3×HA-NUP59* cells in permissive conditions. After incubation in nonpermissive conditions, these cells displayed not only dilated pores (iv) but also large openings in NE (v, arrows). In *nup53Δ nup59Δ GAL-3×HA-POM34* cells, no obvious NPC size abnormalities could be detected both in permissive (vi) and nonpermissive conditions (vii). n, nucleus. Bars: (i–iv, vi, and vii) 100 nm; (v) 500 nm. (B, i–iii) Comparison of pore size distributions in *pom152Δ pom34Δ GAL-3×HA-NUP59* cells (i), *pom152Δ pom34Δ nup53Δ MET3-3×HA-NUP59* cells (ii), and *nup53Δ nup59Δ GAL-3×HA-POM34* cells (iii) incubated in permissive and nonpermissive conditions. (iv) Comparison of pore numbers per section in *nup53Δ nup59Δ GAL-3×HA-POM34* in either permissive or nonpermissive conditions. Gal, galactose medium; dex, dextrose-containing medium; −met, medium lacking methionine; 10× met, medium containing 10× methionine. Error bars indicate SEM.
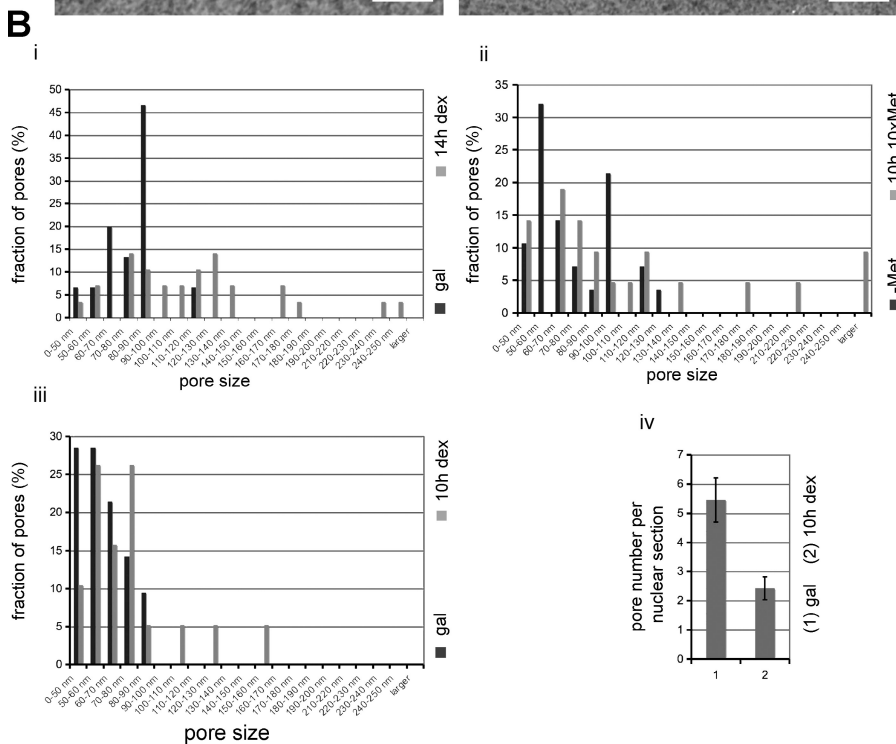
We took advantage of the photoconvertible fluorescent protein Dendra, which irreversibly switches from green to red fluorescence upon the application of a short pulse of UV light (Fig. 8 A; Gurskaya et al., 2006). To test this approach, we fused one of the core nucleoporins, Nup133, with a double Dendra tag (2×Dendra) in wild-type cells and followed its distribution before and after photoconversion. Initially, Nup133-2×Dendra displayed the characteristic punctate nuclear rim distribution, which was detected exclusively in the green channel without any red signal. However, after the application of a short UV pulse, Nup133-2×Dendra was completely photoconverted into the red fluorophore. Over time, newly synthesized Nup133-2×Dendra reemerged in the green channel (Fig. 8 B). The appearance of the green signal was dependent on protein synthesis (unpublished data), demonstrating that Nup133 synthesized before photoconversion was exclusively detected in the red channel
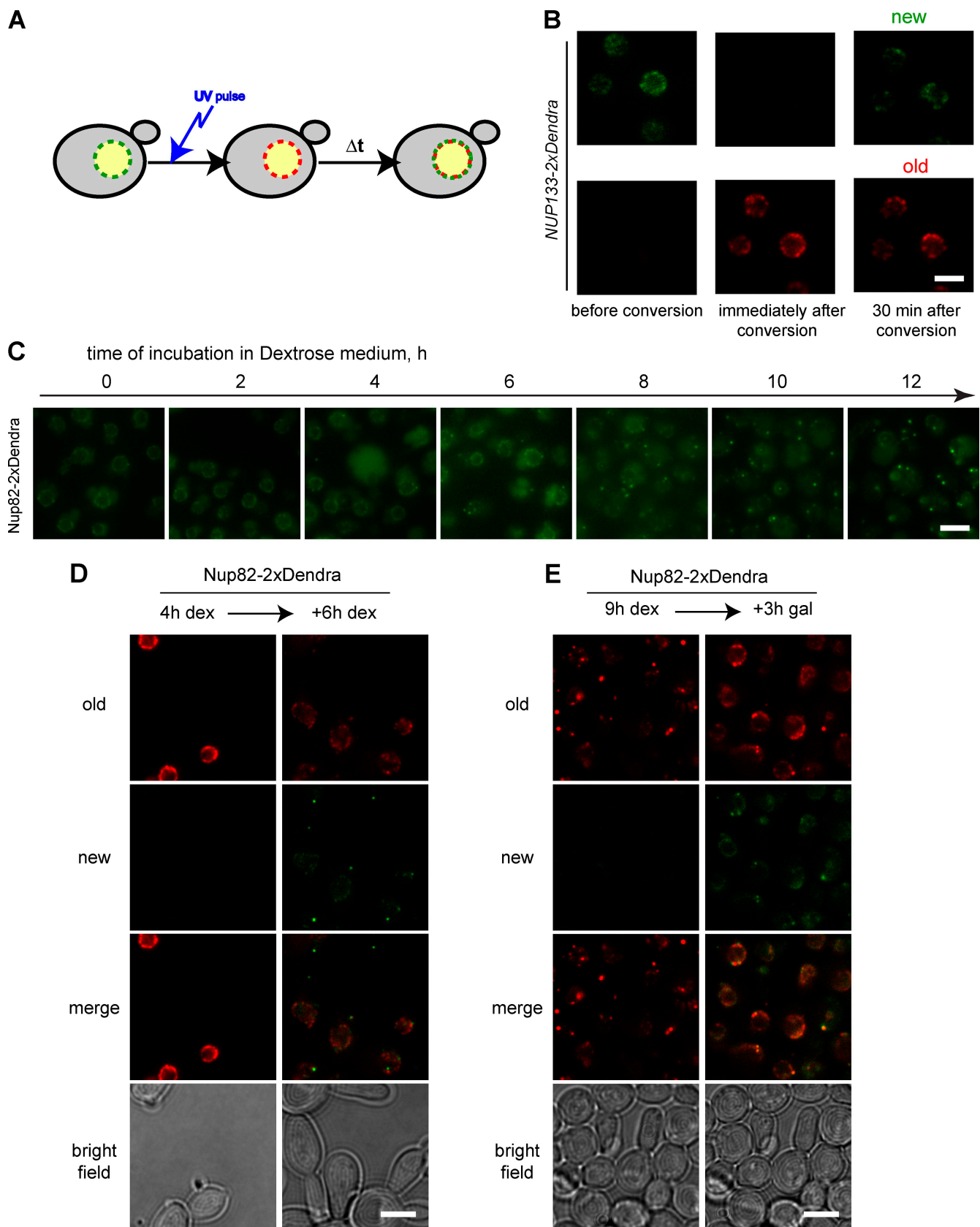
Figure 8. **Dendra assay to analyze distribution of nucleoporins in *nup53Δ nup59Δ GAL-3×HA-POM34* cells.** (A) Representation of the use of Nup-Dendra fusions to track the localization of newly synthesized and preexisting nucleoporins. Initially, Dendra displays green fluorescence but can be irreversibly photoconverted into a red fluorophore by a short pulse of UV light. After conversion, newly made nucleoporins are detected in the green channel, whereas red fluorescence can be used to localize Nups that were synthesized before the photoconversion. (B) Distribution of red and green Nup133-2×Dendra variants before (left), immediately after (middle), and 30 min after photoconversion (right). (C) Time course to visualize the Nup82-Dendra distribution in

and thus could be distinguished from newly made protein. We conclude that the Dendra tag enables separate tracking of old and newly synthesized nucleoporins within single living cells and their progeny.

To examine the origin of mislocalized nucleoporins, we concentrated on Nup82, which displayed the most prominent mislocalization in *nup53Δ nup59Δ* cells upon depletion of Pom34 (Fig. 6 A). As expected, in permissive conditions, Nup82-2×Dendra properly localized to NPCs (Fig. S4 C). A time course analysis revealed that Nup82 started to mislocalize as early as 6 h of incubation in the nonpermissive conditions (Fig. 8 C), but no prominent mislocalization could be detected at the 4-h time point. We therefore preincubated *nup53Δ nup59Δ GAL-3×HA-POM34* cells in dextrose-containing medium for 4 h to initiate depletion of Pom34 and then subjected them to photoconversion (Fig. 8 D, left). After an additional 6-h-long chase period, we observed that newly synthesized Nup82 accumulated almost exclusively in cytoplasmic foci. At the same time, previously synthesized Nup82 was still clearly detectable at the NE (Fig. 8 D, right). This shows that in *nup53Δ nup59Δ* cells, Pom34 is required to efficiently incorporate newly synthesized Nup82 into NPCs, suggesting an NPC assembly defect in these cells.

To test whether the mislocalization of Nup82 is reversible, *NUP82-2×Dendra*–expressing cells were grown in dextrose-containing medium to induce mislocalization of Nup82. Cells were then placed into galactose-containing medium to reinduce *POM34* expression, immediately photoconverted, and reimaged after an additional 3-h chase period (Fig. 8 E). During this chase period, the cytoplasmic foci that contained old Nup82 redistributed into the NE. Furthermore, newly synthesized Nup82 started to correctly localize into nuclear rims (Fig. 8 E). These results suggest that the Pom34-dependent block in NPC formation is reversible and that Nup82, which had accumulated in the cytoplasm, can be chased back into the NE.

Discussion

Characterization of the biochemical interactions of Ndc1

In this study, we have analyzed the physical interactions of the essential yeast transmembrane nucleoporin Ndc1. As summarized in Fig. 9, we found that Ndc1 is embedded into NPC through a web of interactions with at least six nucleoporins, consisting of Pom152, Pom34, Nup59, Nup53, Nup157, and Nup170. Four of these nucleoporins, Pom152, Pom34, Nup53, and Nup59, bind to Ndc1 directly, but we did not find evidence for a direct association between Ndc1 and Nup157 or Nup170. Our purifications demonstrated that Ndc1 forms a stable subcomplex with the other two transmembrane nucleoporins, Pom152 and Pom34. Using cells that lack either Pom152 or Pom34 or express various Pom152 truncations, we show that the integrity of this Ndc1 sub-

complex is dependent on both Pom152 and Pom34 and that the interactions between members of this complex predominantly take place on the cytosolic side of the nuclear membrane (Fig. 1 I). We further show that Pom152 directly binds to Ndc1, but this interaction is clearly weakened in the absence of Pom34 (Fig. 1). This interdependency on both Pom34 and Pom152 for Ndc1 subcomplex formation provides a biochemical explanation for the functional similarity and for the shared set of genetic interactions that was described for both *POM152* and *POM34* (Marelli et al., 1998; Tcheperegine et al., 1999; Miao et al., 2006; this study). Intriguingly, Pom34 and Pom152 were recently isolated in a ring-shaped oligomeric assembly that does not contain Ndc1 (Alber et al., 2007a,b). Based on the biochemical interactions that we describe in this study, it is likely that Ndc1 is also a part of this circular structural unit within NPC. Our experiments further revealed that both Nup59 and Nup53 directly interact with Ndc1, although they compete for binding. The interaction is dependent on the almost identical C-terminal AAHDs within Nup53 and Nup59 (Fig. 2 H), suggesting that these two proteins use the same or highly overlapping binding sites on Ndc1. Although direct interactions of Ndc1 with Nup53 and Nup59 had not been reported previously, it had already been shown that Ndc1 and Pom152 are recruited to proliferated intranuclear membranes that can be observed upon overexpression of Nup53 (Marelli et al., 2001). Using in vitro binding assays, we were unable to detect direct interactions between Ndc1 and Nup157 or Nup170 (unpublished data). However, we observed that Nup53 directly binds to both Nup157 and Nup170, whereas Nup59 directly interacts with Nup170 (Fig. 3), suggesting that Nup53 and Nup59 may act as bridging factors that link Ndc1 to core nucleoporins, in particular to Nup170 and Nup157. In vertebrates, Nup53, the homologue of yeast Nup53/Nup59, was recently shown to interact with the homologue of Ndc1 and with Nup155, the homologue of yeast Nup170/Nup157 (Hawryluk-Gara et al., 2008). Together, these findings point to an evolutionarily conserved set of interactions between Ndc1, Nup157/Nup170, and Nup53/Nup59. It is interesting to note that all four nucleoporins that we identified as direct Ndc1 interaction partners are either transmembrane proteins (Pom152 and Pom34) or have been shown to peripherally associate with membranes (Marelli et al., 2001; Patel and Rexach, 2007). We therefore propose that Ndc1 and its immediate neighbors (Pom152, Pom34, Nup53, and Nup59) constitute the innermost layer of NPC that anchors NPC scaffold elements, including Nup157 and Nup170 to the nuclear pore membrane (Fig. 9).

Biochemical basis for the functional interactions among Ndc1-binding nucleoporins

Our analysis revealed that the genes encoding for proteins that directly interact with Ndc1 are split into two functional elements, which in combination are essential for cell viability. The first

nup53Δ nup59Δ GAL-3×HA-POM34 cells after repression of *POM34* expression without photoconversion. (D) Distribution of newly made and preexisting Nup82-Dendra in *nup53Δ nup59Δ GAL-3×HA-POM34* cells. Cells were incubated for 4 h in nonpermissive conditions, photoconverted (left), and the same field of cells was reimaged after an additional 6-h incubation period (right). (E) Cells were incubated in dextrose medium (dex) for 9 h to induce Nup82 mislocalization, placed in galactose medium (gal), and photoconverted (left). After a 3-h incubation, the same cells were imaged again to detect the distribution of preexisting and newly synthesized Nup82-Dendra. Bars, 5 μm.
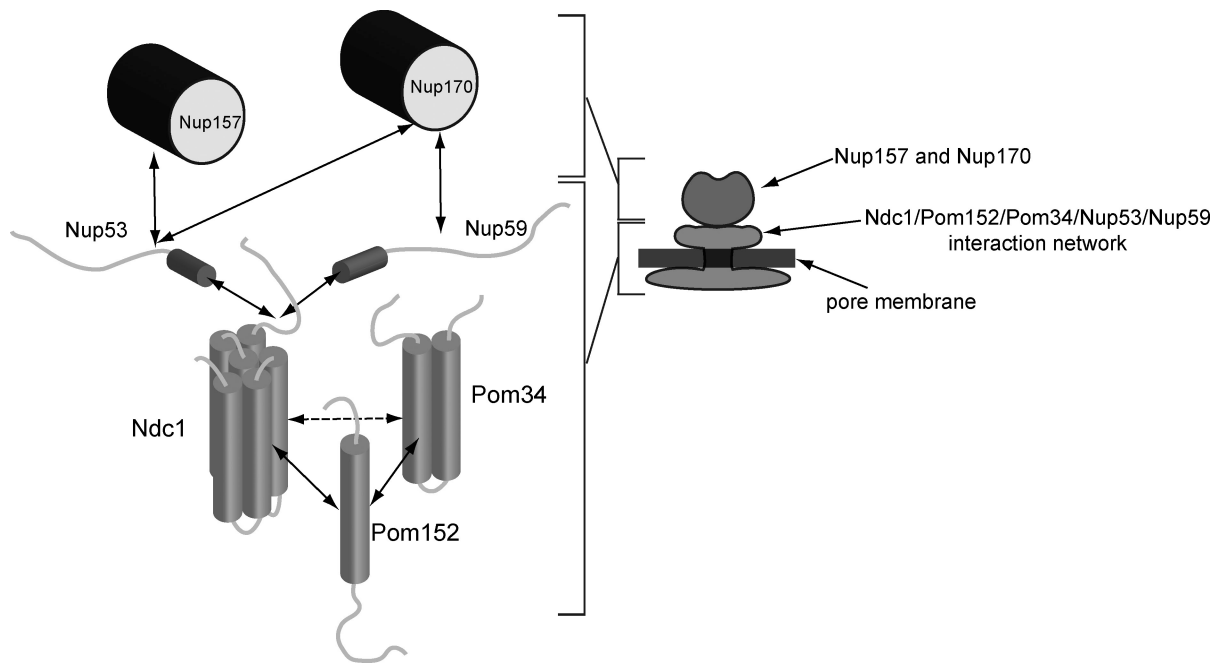
Figure 9. **Summary model of the Ndc1 interaction network.** Solid arrows depict direct protein interactions. The dashed arrow displays the functional requirement of Pom34 for the Ndc1 subcomplex integrity.

element consists of the two transmembrane nucleoporins, *POM152* and *POM34*, which display a synthetic lethal interaction with the second element, which consists of *NUP59* (Table I; Marelli et al., 1998; Tcheperegine et al., 1999; Miao et al., 2006). What is the combined essential function of these two elements? First, Nup59 together with Pom152 and Pom34 plays a redundant role in anchoring and/or targeting of Ndc1 to the NPC (Fig. 4). Second, our biochemical findings suggest that these two functional elements play an important role in bridging the interactions between Ndc1 and other NPC components, in particular Nup170 and Nup157 (Fig. 9). In combination, Nup157 and Nup170 are essential for cell viability (Aitchison et al., 1995) and have a critical function in NPC biogenesis (see Makio et al. on p. 459 of this issue). Interestingly, Nup170 also directly interacts with Pom152 (Makio et al., 2009). It is therefore tempting to speculate that the two groups of Ndc1 interactors may play redundant roles in bridging the interactions between Ndc1 and the essential Nup170/Nup157 pair, thus providing a possible explanation for the genetic interactions that can be observed between the two *POM* genes and *NUP59*. Intriguingly, the filamentous fungus *Aspergillus nidulans* does not contain genes encoding for Nup53, Nup59, or Pom34, and although the homologues of Ndc1 and Pom152 are not required for viability, Nup170 is encoded by an essential gene (Osmani et al., 2006). Therefore, it will be interesting to understand how Nup170 and other core nucleoporins are anchored to the nuclear membrane in this organism.

Nup53 and Nup59 have similar patterns of physical interactions in vitro (Fig. 9) and display some functional redundancy because the loss of both proteins leads to an exacerbated perturbation of NPC structure and function in the *pom152Δ pom34Δ* background when compared with the individual loss of each protein (Fig. 5). However, no synthetic lethal interactions between *NUP53* and the two *POM*s can be detected, and *NUP53*

cannot functionally compensate for the loss of *NUP59* (Table I). This suggests that these two highly related proteins have functionally diverged to play distinct roles at the NPC. Consistent with this, we could detect only Nup59 in the Ndc1 purifications from cell extracts, and only Nup59 conferred efficient recruitment of Ndc1 to the NE in *pom152Δ pom34Δ* mutants (Fig. 4). At present, the molecular basis for the functional differences between Nup59 and Nup53 remains unclear.

Role of Ndc1-interacting nucleoporins in NPC biosynthesis and maintenance

The cell growth phenotypes that we observed upon the loss of the various Ndc1-interacting proteins were accompanied by mislocalization of Ndc1 and other structural nucleoporins, ultrastructural NPC abnormalities, and functional NPC defects. In general, the severity of the NPC defects gradually increased upon the loss of multiple proteins, but collectively, the four Ndc1-interacting proteins appear to be important (a) to connect Ndc1 to other structural elements of NPC, (b) to anchor Ndc1 to the pore, and (c) to maintain the structural integrity of NPC. However, the defects within the different mutants varied, and we found that the conditional depletion of Nup59 (in either *pom152Δ pom34Δ* or *pom152Δ pom34Δ nup53Δ* backgrounds) and the conditional depletion of the Poms (in the *nup59Δ nup53Δ* background) induced distinct phenotypes. For example, in *nup59Δ nup53Δ* cells in which Pom34 was depleted, we observed selective mislocalization of a subset of nucleoporins into cytoplasmic foci. This phenotype was accompanied by a reduction in pore number in the absence of obvious ultrastructural NPC defects (Figs. 6 and 7). To investigate the origin of the mislocalized nucleoporins in these cells, we took advantage of the photoconvertible fluorescent protein Dendra, which enabled us to monitor the intracellular distribution of newly synthesized

and preexisting nucleoporins in parallel (Fig. 8). Using Nup82-Dendra, we showed that upon Pom34 repression in *nup59Δ nup53Δ* cells, newly synthesized Nup82 was almost exclusively localized to cytoplasmic foci. This suggests that newly synthesized Nup82 cannot be incorporated into NPCs and that the process of de novo NPC assembly is blocked in these cells. This conclusion is consistent with the observation that these cells have a reduced number of pores (Fig. 7), as these cells can undergo several rounds of division after the shift to the nonpermissive conditions (e.g., Fig. S2 D) and presumably dilute previously synthesized pores between mother and daughter cells. Interestingly, Makio et al. (2009) also describes defects in new NPC biosynthesis in cells simultaneously lacking Nup170 and Nup157. It is therefore likely that the connection to Nup170 and Nup157 established by Ndc1-interacting proteins is critical for new NPC biosynthesis. Notably, the mislocalization of Nup82 was reversible, and the previously synthesized pool of Nup82 that was present in cytoplasmic foci could be chased back to the NE upon reinduction of Pom34 (Fig. 8). An apparent reversible NPC assembly defect was recently also described in *apq12* mutants (Scarcelli et al., 2007). However, in this case, the defects in NPC assembly were accompanied by invaginations of the inner nuclear membrane, which we did not observe in our strains.

Surprisingly, when we depleted Nup59 in a *pom152Δ pom34Δ* background, we induced a distinct set of phenotypes. Under these conditions, we did not only observe nucleoporin mislocalization but also found severe ultrastructural defects at NPC. Most strikingly, we detected a significant increase in NPC diameter and, in the absence of Nup53, the appearance of large openings within NE, which is reminiscent to the phenotype that we had previously described upon depletion of Ndc1 in the absence of Pom152. Unfortunately, the Dendra assay did not allow us to unambiguously answer the question of whether these enlarged pores represent blocked NPC assembly intermediates or whether they are derived from destabilized pores that have fallen apart. However, *pom152Δ pom34Δ GAL-NUP59* cells display an NPC maintenance defect that can be illustrated with the Dendra assay by the mislocalization of already existing nucleoporins in nonpermissive conditions (Fig. S5). Furthermore, all NPC defects that we observe upon Nup59 depletion are irreversible (unpublished data). Therefore, we favor the hypothesis that in these cells, the stability of NPCs is compromised, which ultimately leads to the disintegration of existing pore structures and the formation of large openings within the NE. Future studies will now be required to analyze the molecular details of how Ndc1 and its interacting partners contribute to NPC assembly and maintenance and to dissect the mechanism of how NPCs are inserted into the lipid bilayers of NE.

Materials and methods

Construction of yeast strains and plasmids
Construction of plasmids for this study (Table S1) was performed using standard molecular cloning techniques. Yeast strains (Table S2) were constructed using either PCR-based transformation approach with specific primers (Longtine et al., 1998), transformation with linearized integration plasmids, or with intact plasmids. Alternatively, yeast mutants were constructed by transformation with genomic regions PCR amplified from the corresponding yeast mutant strains or by mating and subsequent dissection of the tetrads.

Identification of Ndc1-interacting proteins
Pull-downs (Fig. 1 A) were performed using a modification of the protocol described in Carvalho et al. (2006). Cells from 300 ml of culture grown to $OD_{600} = 2.5$ were harvested, washed, and subsequently lysed in lysis buffer (LB; 0.1 M Hepes, pH 7.5, 0.3 M KCl, 0.2 mM EDTA, 10 mM EGTA, 20 mM MgOAc, and 10 mM β-mercaptoethanol) in the presence of protease inhibitors using a mini-bead beater (BioSpec Products, Inc.). To prepare crude membrane fractions, the extracts were first subjected to a low-speed centrifugation to remove large cell debris and nonlysed cells followed by high-speed centrifugation (16,000 rpm; SS-34 rotor; Sorvall) for 30 min to pellet membranes. The membranes were extracted in 1.5 ml ice-cold LB/inhibitors plus 1% digitonin (final concentration), and soluble fractions were incubated for 1.5 h at 4°C with 100 µl S protein–conjugated agarose beads (S beads; EMD). Beads were extensively washed, and bound proteins were eluted by 5 min boiling with SDS sample buffer diluted 1:3 with distilled water and separated by SDS-PAGE. Proteins were visualized with GelCode staining reagent (Bio-Rad Laboratories), and the desired areas differing in protein content were excised from the gel and identified by matrix-assisted laser desorption/ionization time of flight MS and LC-MS/MS.

Characterization of the interactions between Ndc1, Pom152, and Pom34
The analytical TAP-tagged affinity pull-downs (Fig. 1, B–D and G) were performed using a procedure similar to the aforementioned one using S beads. Eluted proteins were separated by SDS-PAGE and visualized with SYPRO-Ruby (Invitrogen) using a UV transilluminator coupled to a digital camera (Alpha Innotech). Conditions for TAP-tagged pull-downs at a lower salt concentration (Fig. 1 B) were identical except that experiments were performed in LB diluted 1:1 with distilled water. For Western blotting experiments (Fig. 1 F), digitonin was added to 1 ml bead beater cell lysate up to a final concentration of 1%, and after 10 min incubation on ice, the solubilized material was clarified by 2 min centrifugation at 10,000 rpm in a tabletop mini centrifuge. The extract was incubated for 1 h with 20 µl S beads. The beads were washed and eluted with SDS sample buffer. After resolving by SDS-PAGE, the proteins were blotted onto nitrocellulose membranes and probed with the respective primary and secondary antibodies.

Purification of recombinant proteins and preparation of bacterial cell extract
Cultures of *E. coli* BL-21 cells transformed with the respective protein-coding plasmids were induced with 0.5 mM IPTG for 2 h at RT. Cells were harvested by centrifugation and lysed by sonication in 1:20 culture volume of LB (PBS, pH 7.4, 1 mM PMSF, and 5 mM DTT) for GST fusions and (50 mM Na-phosphate, pH 7.5, 300 mM NaCl, 1 mM PMSF, and 5 mM β-mercaptoethanol) for 6×His-MBP fusions. Lysates were supplied with 1% Triton X-100 (final concentration) for GST fusions or 0.5% Triton X-100 for 6×His-MBP fusions and clarified by 10 min centrifugation at 12,000 rpm (SS-34 rotor). Supernatants were incubated with either Sepharose-GSH beads (GE Healthcare) or His-Select affinity beads (Sigma-Aldrich). Beads were washed with wash buffer (PBS, pH 7.4, 0.1 mM DTT, and 0.1% Tween 20) for GST fusions or (50 mM Na-phosphate, pH 7.5, 300 mM NaCl, 1 mM β-mercaptoethanol, and 0.1% Tween 20) for 6×His-MBP fusions and eluted with either glutathione elution buffer (75 mM Tris-HCl, pH 8.1, and 10 mM GSH) or with His-tag elution buffer (50 mM Na-phosphate, pH 7.5, 300 mM NaCl, and 200 mM imidazole).

Preparation of Ndc1-TAP, TAP-Nup170, and TAP-Nup157 beads
Yeast cells conferring galactose-inducible overexpression of Ndc1-TAP (KWY2028) were grown in medium containing 2% dextrose, washed, and diluted into medium containing 2% galactose to induce Ndc1-TAP overexpression. Cells were grown overnight and harvested, washed, and lysed in LB containing protease inhibitors in a preparative scale bead beater (BioSpec Products, Inc.). Cell debris was removed from the lysate by centrifugation (5 min at 2,000 rpm in a tabletop centrifuge), and membranes were collected by high-speed centrifugation at 17,000 rpm (SS-34 rotor) for 1 h. The membrane pellet was diluted with ice-cold LB/inhibitors, frozen in liquid N_2 in 1-ml aliquots, and stored at −70°C. For preparation of Ndc1-TAP S beads, aliquots of the membrane suspension were diluted 1:1 with LB plus protease inhibitors and 1.2% octyl-D-glucopyranoside (final concentration), incubated for 20 min, and clarified by a 10,000 rpm centrifugation in a tabletop mini centrifuge. To immobilize Ndc1-TAP, the supernatant

was then incubated with S beads. Alternatively, Ndc1-TAP membranes were solubilized with 0.5% Triton X-100 and washed with LB plus 0.1% Tween 20. The Triton extraction protocol provided better efficiency of Ndc1 immobilization, although the protein appeared to be less active in the in vitro binding experiments when compared with the octyl-D-glucopyranoside extraction procedure. The overexpression of TAP-Nup157 (KWY2377) and TAP-Nup170 (KWY2378) was similar as described for Ndc1-TAP. Lysis was performed using glass beads with ice-cold LB/inhibitors supplemented with 1% Triton X-100 (final concentration). Insoluble cell debris was removed by 5-min 4,500 rpm centrifugation in a tabletop centrifuge, and the supernatant was incubated with S beads and extensively washed with LB supplemented with 0.1% Tween 20.

In vitro binding assays with Nup53, Nup59, Ndc1, Nup157, and Nup170

For each in vitro binding reaction, aliquots of the bait protein were premixed with an equal volume of LB or LB containing bacterial proteins in the presence of 10% glycerol and 0.4% digitonin, and protein mixtures were added to preequilibrated beads. For competition assays (Fig. 2, F and G), beads were first preincubated with an excess of competitor protein solution followed by the addition of the respective full-length protein. Beads were briefly washed and eluted with high salt elution buffer (1.25 M NaCl, 50 mM Hepes-KOH, pH 7.5, and 0.2% digitonin). Eluted proteins were precipitated with methanol-chloroform, separated by SDS-PAGE, and stained with SYPRO-Ruby. The remaining beads were also subjected to a second stringent elution with ammonium hydroxide (Oeffinger et al., 2007) to exclude the possibility that the binding of some proteins was not detected because they resisted salt elution. The ammonium hydroxide eluates were dried in a Speedvac (GMI, Inc.) and resolubilized in SDS sample buffer before separation by SDS-PAGE.

Fluorescence microscopy

Cells were grown at 30°C in permissive synthetic selection media (containing galactose or containing dextrose and lacking methionine) or in the nonpermissive synthetic selection media (containing dextrose or containing dextrose and 0.2 mg/ml methionine). The media were supplemented with twofold excess of adenine, and cell density was kept under OD_{600} = 0.5 to reduce autofluorescence. For all live imaging experiments except for color Dendra assays, cells were concentrated by centrifugation, mounted under a cover slide in culture media, and imaged directly. All Images were acquired with a digital camera (CA742-98; Hamamatsu Photonics) controlled by the Metamorph software program (MDS Analytical Technologies). Images were processed using Photoshop (CS2; Adobe), and figures were assembled using Photoshop and Illustrator (CS2; Adobe).

For depletion Dendra experiments, cells were grown overnight in the permissive media essentially as described in the previous paragraph and diluted into the nonpermissive media. Cells were collected for Dendra microscopy at the times specified in Figs. 8 and S5. Cells were washed with fresh medium and concentrated during the final wash step. 2 µl cells was placed on a 2% low melt agarose pad prepared using respective medium. Dendra was converted by 4 × 20–ms pulses of UV light in DAPI channel followed by 8 s YFP exposure to bleach remaining signal. Slides were incubated at 30°C between time points. For recovery experiments, cells were grown in nonpermissive conditions for the time stated in Fig. 8. Cells were washed three times with 500 µl of the permissive media, and 2 µl was placed on an agarose pad prepared using the permissive media. Cells were imaged immediately, incubated at 30°C for the time stated in Fig. 8, and imaged again. Dendra was converted with one 20-ms UV exposure followed by a 10-s YFP exposure to bleach remaining signal. After the chase period, the same field of cells was imaged again in rhodamine and YFP channels.

Ultrastructural analysis

The EM analysis of yeast mutants was performed essentially as described in Madrid et al. (2006).

Online supplemental material

Fig. S1 shows the localization of Ndc1 and Pom34 in strains expressing myc-tagged Pom152 variants and provides additional analyses of the protein interactions of Ndc1. Fig. S2 shows the growth of the various deletion and depletion strains used in this study. Fig. S3 illustrates the functionality of the tagged Ndc1 variants used in this study. Fig. S4 shows the localization of different reporter proteins in various mutants affecting the Ndc1 network. Fig. S5 shows the distribution of old and new Nup133-Dendra protein in *pom152Δ pom34Δ GAL-3×HA-NUP59* cells upon depletion of Nup59. Tables S1 and S2 describe the plasmids and yeast strains used in this study. Online supplemental material is available at http://www.jcb .org/cgi/content/full/jcb.200810030/DC1.

References

Aitchison, J.D., M.P. Rout, M. Marelli, G. Blobel, and R.W. Wozniak. 1995. Two novel related yeast nucleoporins Nup170p and Nup157p: complementation with the vertebrate homologue Nup155p and functional interactions with the yeast nuclear pore-membrane protein Pom152p. *J. Cell Biol.* 131:1133–1148.

Alber, F., S. Dokudovskaya, L.M. Veenhoff, W. Zhang, J. Kipper, D. Devos, A. Suprapto, O. Karni-Schmidt, R. Williams, B.T. Chait, et al. 2007a. Determining the architectures of macromolecular assemblies. *Nature.* 450:683–694.

Alber, F., S. Dokudovskaya, L.M. Veenhoff, W. Zhang, J. Kipper, D. Devos, A. Suprapto, O. Karni-Schmidt, R. Williams, B.T. Chait, et al. 2007b. The molecular architecture of the nuclear pore complex. *Nature.* 450:695–701.

Antonin, W., C. Franz, U. Haselmann, C. Antony, and I.W. Mattaj. 2005. The integral membrane nucleoporin pom121 functionally links nuclear pore complex assembly and nuclear envelope formation. *Mol. Cell.* 17:83–92.

Antonin, W., J. Ellenberg, and E. Dultz. 2008. Nuclear pore complex assembly through the cell cycle: regulation and membrane organization. *FEBS Lett.* 582:2004–2016.

Beck, M., F. Forster, M. Ecke, J.M. Plitzko, F. Melchior, G. Gerisch, W. Baumeister, and O. Medalia. 2004. Nuclear pore complex structure and dynamics revealed by cryoelectron tomography. *Science.* 306:1387–1390.

Beck, M., V. Lucic, F. Forster, W. Baumeister, and O. Medalia. 2007. Snapshots of nuclear pore complexes in action captured by cryo-electron tomography. *Nature.* 449:611–615.

Belgareh, N., G. Rabut, S.W. Bai, M. van Overbeek, J. Beaudouin, N. Daigle, O.V. Zatsepina, F. Pasteau, V. Labas, M. Fromont-Racine, et al. 2001. An evolutionarily conserved NPC subcomplex, which redistributes in part to kinetochores in mammalian cells. *J. Cell Biol.* 154:1147–1160.

Berke, I.C., T. Boehmer, G. Blobel, and T.U. Schwartz. 2004. Structural and functional analysis of Nup133 domains reveals modular building blocks of the nuclear pore complex. *J. Cell Biol.* 167:591–597.

Brohawn, S.G., N.C. Leksa, E.D. Spear, K.R. Rajashankar, and T.U. Schwartz. 2008. Structural evidence for common ancestry of the nuclear pore complex and vesicle coats. *Science.* 322:1369–1373.

Carvalho, P., V. Goder, and T.A. Rapoport. 2006. Distinct ubiquitin-ligase complexes define convergent pathways for the degradation of ER proteins. *Cell.* 126:361–373.

Chial, H.J., M.P. Rout, T.H. Giddings, and M. Winey. 1998. *Saccharomyces cerevisiae* Ndc1p is a shared component of nuclear pore complexes and spindle pole bodies. *J. Cell Biol.* 143:1789–1800.

Cronshaw, J.M., A.N. Krutchinsky, W. Zhang, B.T. Chait, and M.J. Matunis. 2002. Proteomic analysis of the mammalian nuclear pore complex. *J. Cell Biol.* 158:915–927.

D'Angelo, M.A., and M.W. Hetzer. 2006. The role of the nuclear envelope in cellular organization. *Cell. Mol. Life Sci.* 63:316–332.

Dultz, E., E. Zanin, C. Wurzenberger, M. Braun, G. Rabut, L. Sironi, and J. Ellenberg. 2008. Systematic kinetic analysis of mitotic dis- and reassembly of the nuclear pore in living cells. *J. Cell Biol.* 180:857–865.

Franz, C., R. Walczak, S. Yavuz, R. Santarella, M. Gentzel, P. Askjaer, V. Galy, M. Hetzer, I.W. Mattaj, and W. Antonin. 2007. MEL-28/ELYS is required for the recruitment of nucleoporins to chromatin and postmitotic nuclear pore complex assembly. *EMBO Rep.* 8:165–172.

Gilbert, W., C.W. Siebel, and C. Guthrie. 2001. Phosphorylation by Sky1p promotes Npl3p shuttling and mRNA dissociation. *RNA.* 7:302–313.

Gillespie, P.J., G.A. Khoudoli, G. Stewart, J.R. Swedlow, and J.J. Blow. 2007. ELYS/MEL-28 chromatin association coordinates nuclear pore complex assembly and replication licensing. *Curr. Biol.* 17:1657–1662.

Gurskaya, N.G., V.V. Verkhusha, A.S. Shcheglov, D.B. Staroverov, T.V. Chepurnykh, A.F. Fradkov, S. Lukyanov, and K.A. Lukyanov. 2006.

Engineering of a monomeric green-to-red photoactivatable fluorescent protein induced by blue light. *Nat. Biotechnol.* 24:461–465.

Hallberg, E., R.W. Wozniak, and G. Blobel. 1993. An integral membrane protein of the pore membrane domain of the nuclear envelope contains a nucleoporin-like region. *J. Cell Biol.* 122:513–521.

Harel, A., A.V. Orjalo, T. Vincent, A. Lachish-Zalait, S. Vasu, S. Shah, E. Zimmerman, M. Elbaum, and D.J. Forbes. 2003. Removal of a single pore subcomplex results in vertebrate nuclei devoid of nuclear pores. *Mol. Cell.* 11:853–864.

Hawryluk-Gara, L.A., M. Platani, R. Santarella, R.W. Wozniak, and I.W. Mattaj. 2008. Nup53 is required for nuclear envelope and nuclear pore complex assembly. *Mol. Biol. Cell.* 19:1753–1762.

Hetzer, M.W., T.C. Walther, and I.W. Mattaj. 2005. Pushing the envelope: structure, function, and dynamics of the nuclear periphery. *Annu. Rev. Cell Dev. Biol.* 21:347–380.

Hinshaw, J.E., B.O. Carragher, and R.A. Milligan. 1992. Architecture and design of the nuclear pore complex. *Cell.* 69:1133–1141.

Hodel, A.E., M.R. Hodel, E.R. Griffis, K.A. Hennig, G.A. Ratner, S. Xu, and M.A. Powers. 2002. The three-dimensional structure of the autoproteolytic, nuclear pore-targeting domain of the human nucleoporin Nup98. *Mol. Cell.* 10:347–358.

Hsia, K.C., P. Stavropoulos, G. Blobel, and A. Hoelz. 2007. Architecture of a coat for the nuclear pore membrane. *Cell.* 131:1313–1326.

Jaspersen, S.L., T.H. Giddings Jr., and M. Winey. 2002. Mps3p is a novel component of the yeast spindle pole body that interacts with the yeast centrin homologue Cdc31p. *J. Cell Biol.* 159:945–956.

Jeudy, S., and T.U. Schwartz. 2007. Crystal structure of nucleoporin Nic96 reveals a novel, intricate helical domain architecture. *J. Biol. Chem.* 282:34904–34912.

Longtine, M.S., A. McKenzie III, D.J. Demarini, N.G. Shah, A. Wach, A. Brachat, P. Philippsen, and J.R. Pringle. 1998. Additional modules for versatile and economical PCR-based gene deletion and modification in *Saccharomyces cerevisiae*. *Yeast.* 14:953–961.

Madrid, A.S., J. Mancuso, W.Z. Cande, and K. Weis. 2006. The role of the integral membrane nucleoporins Ndc1p and Pom152p in nuclear pore complex assembly and function. *J. Cell Biol.* 173:361–371.

Makio, T., L.H. Stanton, C.-C. Lin, D.S. Goldfarb, K. Weis, and R.W. Wozniak. 2009. The nucleoporins Nup170p and Nup157p are essential for nuclear pore complex assembly. *J. Cell Biol.* 185:459–473.

Mansfeld, J., S. Guttinger, L.A. Hawryluk-Gara, N. Pante, M. Mall, V. Galy, U. Haselmann, P. Muhlhausser, R.W. Wozniak, I.W. Mattaj, et al. 2006. The conserved transmembrane nucleoporin NDC1 is required for nuclear pore complex assembly in vertebrate cells. *Mol. Cell.* 22:93–103.

Marelli, M., J.D. Aitchison, and R.W. Wozniak. 1998. Specific binding of the karyopherin Kap121p to a subunit of the nuclear pore complex containing Nup53p, Nup59p, and Nup170p. *J. Cell Biol.* 143:1813–1830.

Marelli, M., C.P. Lusk, H. Chan, J.D. Aitchison, and R.W. Wozniak. 2001. A link between the synthesis of nucleoporins and the biogenesis of the nuclear envelope. *J. Cell Biol.* 153:709–724.

Maul, G.G., H.M. Maul, J.E. Scogna, M.W. Lieberman, G.S. Stein, B.Y. Hsu, and T.W. Borun. 1972. Time sequence of nuclear pore formation in phytohemagglutinin-stimulated lymphocytes and in HeLa cells during the cell cycle. *J. Cell Biol.* 55:433–447.

McDonald, K., and T. Muller-Reichert. 2002. Cryomethods for thin section electron microscopy. *Methods Enzymol.* 351:96–123.

Melcak, I., A. Hoelz, and G. Blobel. 2007. Structure of Nup58/45 suggests flexible nuclear pore diameter by intermolecular sliding. *Science.* 315:1729–1732.

Miao, M., K.J. Ryan, and S.R. Wente. 2006. The integral membrane protein Pom34p functionally links nucleoporin subcomplexes. *Genetics.* 172:1441–1457.

Oeffinger, M., K.E. Wei, R. Rogers, J.A. Degrasse, B.T. Chait, J.D. Aitchison, and M.P. Rout. 2007. Comprehensive analysis of diverse ribonucleoprotein complexes. *Nat. Methods.* 4:951–956.

Osmani, A.H., J. Davies, H.L. Liu, A. Nile, and S.A. Osmani. 2006. Systematic deletion and mitotic localization of the nuclear pore complex proteins of *Aspergillus nidulans*. *Mol. Biol. Cell.* 17:4946–4961.

Patel, S.S., and M.F. Rexach. 2007. Discovering novel interactions at the nuclear pore complex using Bead Halo: A rapid method for detecting molecular interactions of high and low affinity at equilibrium. *Mol. Cell. Proteomics.* 7:121–131.

Rabut, G., P. Lenart, and J. Ellenberg. 2004. Dynamics of nuclear pore complex organization through the cell cycle. *Curr. Opin. Cell Biol.* 16:314–321.

Rasala, B.A., A.V. Orjalo, Z. Shen, S. Briggs, and D.J. Forbes. 2006. ELYS is a dual nucleoporin/kinetochore protein required for nuclear pore assembly and proper cell division. *Proc. Natl. Acad. Sci. USA.* 103:17801–17806.

Rout, M.P., J.D. Aitchison, A. Suprapto, K. Hjertaas, Y. Zhao, and B.T. Chait. 2000. The yeast nuclear pore complex: composition, architecture, and transport mechanism. *J. Cell Biol.* 148:635–651.

Scarcelli, J.J., C.A. Hodge, and C.N. Cole. 2007. The yeast integral membrane protein Apq12 potentially links membrane dynamics to assembly of nuclear pore complexes. *J. Cell Biol.* 178:799–812.

Schrader, N., P. Stelter, D. Flemming, R. Kunze, E. Hurt, and I.R. Vetter. 2008. Structural basis of the nic96 subcomplex organization in the nuclear pore channel. *Mol. Cell.* 29:46–55.

Siebel, C.W., and C. Guthrie. 1996. The essential yeast RNA binding protein Np13p is methylated. *Proc. Natl. Acad. Sci. USA.* 93:13641–13646.

Stavru, F., B.B. Hulsmann, A. Spang, E. Hartmann, V.C. Cordes, and D. Gorlich. 2006a. NDC1: a crucial membrane-integral nucleoporin of metazoan nuclear pore complexes. *J. Cell Biol.* 173:509–519.

Stavru, F., G. Nautrup-Pedersen, V.C. Cordes, and D. Gorlich. 2006b. Nuclear pore complex assembly and maintenance in POM121- and gp210-deficient cells. *J. Cell Biol.* 173:477–483.

Suntharalingam, M., and S.R. Wente. 2003. Peering through the pore. Nuclear pore complex structure, assembly, and function. *Dev. Cell.* 4:775–789.

Tcheperegine, S.E., M. Marelli, and R.W. Wozniak. 1999. Topology and functional domains of the yeast pore membrane protein Pom152p. *J. Biol. Chem.* 274:5252–5258.

Tran, E.J., and S.R. Wente. 2006. Dynamic nuclear pore complexes: life on the edge. *Cell.* 125:1041–1053.

Unwin, P.N., and R.A. Milligan. 1982. A large particle associated with the perimeter of the nuclear pore complex. *J. Cell Biol.* 93:63–75.

Walther, T.C., A. Alves, H. Pickersgill, I. Loiodice, M. Hetzer, V. Galy, B.B. Hulsmann, T. Kocher, M. Wilm, T. Allen, et al. 2003. The conserved Nup107-160 complex is critical for nuclear pore complex assembly. *Cell.* 113:195–206.

Weirich, C.S., J.P. Erzberger, J.M. Berger, and K. Weis. 2004. The N-terminal domain of Nup159 forms a beta-propeller that functions in mRNA export by tethering the helicase Dbp5 to the nuclear pore. *Mol. Cell.* 16:749–760.

Winey, M., D. Yarar, G.T.H. Jr, and D.N. Mastronarde. 1997. Nuclear pore complex number and distribution throughout the *Saccharomyces cerevisiae* cell cycle by three-dimensional reconstruction from electron micrographs of nuclear envelopes. *Mol. Biol. Cell.* 8:2119–2132.

Wozniak, R.W., and G. Blobel. 1992. The single transmembrane segment of gp210 is sufficient for sorting to the pore membrane domain of the nuclear envelope. *J. Cell Biol.* 119:1441–1449.

Wozniak, R.W., G. Blobel, and M.P. Rout. 1994. POM152 is an integral protein of the pore membrane domain of the yeast nuclear envelope. *J. Cell Biol.* 125:31–42.

Yang, Q., M.P. Rout, and C.W. Akey. 1998. Three-dimensional architecture of the isolated yeast nuclear pore complex: functional and evolutionary implications. *Mol. Cell.* 1:223–234.